การวิเคราะห์ปริมาณโปรตีนในน้ำนมโดยวิธีคัลเลอริเมตริกด้วยอนุภาคระดับนาโนเมตรของทองคำ

นายสรรพล วันทาศิลป์

วิทยานิพนธ์นี้เป็นส่วนหนึ่งของการศึกษาตามหลักสูตรปริญญาวิทยาศาสตรมหาบัณฑิต
สาขาวิชาเคมี ภาควิชาเคมี
คณะวิทยาศาสตร์ จุฬาลงกรณ์มหาวิทยาลัย
ปีการศึกษา 2554

GOLD NANOPARTICLE-BASED COLORIMETRIC ANALYSIS OF PROTEIN CONTENT IN MILK

Mr. Sanpon Vantasin

A Thesis Submitted in Partial Fulfillment of the Requirements

for the Degree of Master of Science Program in Chemistry

Department of Chemistry

Faculty of Science

Chulalongkorn University

Academic Year 2011

Thesis Title	GOLD NANOPARTICLE-BASED COLORIMETRIC ANALYSIS OF PROTEIN CONTENT IN MILK
By	Mr. Sanpon Vantasin
Field of Study	Chemistry
Thesis Advisor	Associate Professor Sanong Ekgasit, Ph.D.
Thesis Co-advisor	Associate Professor Chuchaat Thammacharoen

Accepted by the Faculty of Science, Chulalongkorn University in Partial Fulfillment of the Requirements for Master's degree

……. Dean of the Faculty of Science
(Professor Supot Hannongbua, Ph.D.)

THESIS COMMITTEE

…… Chairman
(Associate Professor Warinthorn Chavasiri, Ph.D.)

…… Thesis Advisor
(Associate Professor Sanong Ekgasit, Ph.D.)

…… Thesis Co-Advisor
(Associate Professor Chuchaat Thammacharoen)

…… Examiner
(Lecturer Numpon Insin, Ph.D.)

…… External Examiner
(Associate Professor Chinapong Kritayakornupong, Ph.D.)

สรรพล วันทาศิลป์ : การวิเคราะห์ปริมาณโปรตีนในน้ำนมโดยวิธีคัลเลอริเมตริกด้วยอนุภาคระดับนาโนเมตรของทองคำ (GOLD NANOPARTICLE-BASED COLORIMETRIC ANALYSIS OF PROTEIN CONTENT IN MILK) อ.ที่ปรึกษาวิทยานิพนธ์หลัก: รศ. ดร. สนอง เอกสิทธิ์, อ.ที่ปรึกษาวิทยานิพนธ์ร่วม: รศ.ชูชาติ ธรรมเจริญ, 55 หน้า.

งานวิจัยนี้ได้พัฒนาการวิเคราะห์ปริมาณโปรตีนในน้ำนมด้วยวิธีคัลเลอริเมตริกที่สามารถทำได้ง่าย วิธีการนี้อาศัยความสามารถในการช่วยเสถียรของโปรตีนซึ่งสามารถยับยั้งการจับตัวกันของอนุภาคระดับนาโนเมตรของทองคำที่ถูกกระตุ้นโดยกรดไฮโดรคลอริกได้ โดยเมื่อมีโปรตีนของน้ำนมอยู่ในระบบ วิธีการวิเคราะห์จะให้ผลเป็นสีแดงจนถึงสีน้ำเงินอย่างชัดเจน ตามความเข้มข้นของโปรตีน เนื่องจากสีที่เกิดขึ้นซึ่งเป็นผลจากปรากฏการณ์โลคัลไลซ์เซอร์เฟสพลาสมอนเรโซแนนซ์ นั้นสามารถสังเกตผลได้ด้วยตาเปล่าและยูวี-วิซิเบิล สเปกโทรสโกปี จึงทำให้สามารถวิเคราะห์ปริมาณโปรตีนในตัวอย่างได้ ในเงื่อนไขของระบบที่เหมาะสมวิธีการวิเคราะห์นี้จะมีสภาพไวสูงมากจนสามารถแยกแยะความเข้มข้นของโปรตีนที่ใกล้เคียงกันแม้ต่างกันไม่ถึงสิบเท่าได้ด้วยการสังเกตผลด้วยตาเปล่า โดยมีช่วงที่ไวต่อการวิเคราะห์ซึ่งสามารถปรับได้ในช่วง 2.93×10^{-1} ถึง 2.93×10^{-3} มิลลิกรัมต่อมิลลิลิตร ในการวิเคราะห์เดียวกันยังสามารถเพิ่มความแม่นยำได้โดยใช้ยูวี-วิซิเบิล สเปกโทรสโกปีเพื่อตรวจวัดค่าความยาวคลื่นที่การดูดกลืนสูงสุด หรืออัตราส่วนระหว่างค่าการดูดกลืนที่สูงสุดกับที่ 520 นาโนเมตร การทดสอบกับสิ่งเจือปนยังแสดงให้เห็นว่าวิธีการวิเคราะห์นี้ไม่สามารถถูกลวงด้วยแป้ง น้ำตาลแลคโตส น้ำตาลทราย เมลามีน หรือโซเดียมคลอไรด์ได้ วิธีการวิเคราะห์ที่พัฒนาขึ้นนี้เรียบง่ายมาก ใช้เวลาในการวิเคราะห์เพียง 6 นาที และไม่จำเป็นต้องทำการสกัดสารตัวอย่าง

ภาควิชา เคมี ลายมือชื่อนิสิต .....

สาขาวิชา เคมี ลายมือชื่อ อ.ที่ปรึกษาวิทยานิพนธ์หลัก .....

ปีการศึกษา 2554 ลายมือชื่อ อ.ที่ปรึกษาวิทยานิพนธ์ร่วม .....

5372351823 : MAJOR CHEMISTRY
KEYWORDS : GOLD NANOPARTICLES / MILK / PROTEIN DETERMINATION

SANPON VANTASIN : GOLD NANOPARTICLE-BASED COLORIMETRIC ANALYSIS OF PROTEIN CONTENT IN MILK. ADVISOR: ASSOC. PROF. SANONG EKGASIT, Ph.D., CO-ADVISOR: ASSOC. PROF. CHUCHAAT THAMMACHAROEN, 55 pp.

An easy-to-practice colorimetric analysis of milk protein content has been developed. The assay relies on stabilization power of protein that can inhibit gold nanoparticles (AuNPs) aggregation induced by hydrochloric acid. In the presence of milk protein, the assay gave explicit red to blue color depending on protein concentration. Since the appeared colors, which emerge from localized surface plasmon resonance phenomenon, can be observed by naked-eye sensing or UV-visible spectroscopy, protein concentration of the sample could be evaluated. With the optimized condition, the assay is so sensitive that it can distinguish nearby protein concentrations in the same order of magnitude by naked eye sensing with adjustable sensitive range in 2.93×10^{-1} to 2.93×10^{-3} mg/mL. In the assay, extra accuracy can be achieved using UV-visible spectroscopy to measure λ_{max} or intensity ratio at maxima and at 520 nm. Interfering substance study showed that starch, lactose, table sugar, melamine, and sodium chloride cannot deceive the assay. The developed assay is very simple, requires only 6 minutes analysis time and does not need extraction process.

Department of Study: Chemistry Student's Signature .....
Field of Study: Chemistry Advisor's Signature .....
Academic Year: 2011 Co-advisor's Signature .....

ACKNOWLEDGEMENTS

I would like to wholeheartedly express my gratitude to my advisor, Associate Professor Dr. Sanong Ekgasit and co-advisor Associate Professor Chuchaat Thammacharoen for many useful advice, sincere suggestions, and detailed instructions in both fundamental knowledge and laboratory techniques.

I would like to thank Assistant Professor Dr. Warinthorn Chavasiri, Dr. Numpon Insin, and Associate Professor Dr. Chinapong Kritayakornupong for being my thesis committee with a lot of kind and useful suggestions. Their comments about theoretical concepts and grammars in my thesis writing really helped me a lot.

I also give my thank for my research group: Sensor Research Unit, Department of Chemistry, Faculty of Science, Chulalongkorn Universitiy for providing abundant laboratory instruments in the research. The gratitude also goes to my colleagues in the group who give me a lot of suggestions, ideas, and encouragements when I need some.

This research has financial support from Center of Innovative Nanotechnology Chulalongkorn University (CIN-CU) and National Center of Excellence for Petroleum, Petrochemicals, and Advance Materials (CE-PPAM).

If there are some mistakes or blunders in this thesis, they are the sole responsibility of me.

Above all, I give the credit of everything I have done to my parents and my Lord Jesus Christ, who give me true love that nothing can replace.

CONTENTS

Page

LIST OF FIGURES

Figure Page

LIST OF ABBREVIATIONS & SYMBOLS

AuNPs	: gold nanoparticles
$HAuCl_4$	: chloroauric acid
HCl	: hydrochloric acid
HNO_3	: nitric acid
NaOH	: sodium hydroxide
λ_{max}	: wavelength at maxima absorption/extinction
nm	: nanometer
g	: gram
mg	: milligram
mL	: milliliter
M	: molar
ppm	: part per million
°C	: degree celsius
UV-visible	: ultraviolet-visible
FT-IR	: fourier transfrom infrared
TEM	: transmission electron microscopy
DI water	: deionized water

CHAPTER I

INTRODUCTION

1.1 MILK ISSUE IN THAILAND

As one of the most important agricultural products of the country, more than nine hundred thousands tons of milk was produced in Thailand in 2011 [1]. With its low price and ease of consumption, milk is a crucial protein source for the citizen especially for the youths. The government emphasized this importance by establishing 'school milk project' in 1992 to provide free milk in kindergartens and elementary schools with the objective of improving health of young students. The project gave rise to new milk producers, which intensified the competition in milk market that was already high. Additionally, numerous corruption cases in the project were reported every year [2]. In 2009, these incidents dissipated most of 13.6 billon baht assigned to the project away and only 1.5 billion baht was paid to the manufacturers [3-4]. This problem pressured milk producers to reduce the cost of production to be still profitable. Many producers did this by unrighteous methods such as cutting down quality control or milk counterfeiting. There are many research reports about milk manufacturers and suppliers which do not meet the standard [5-6]. Many cases of counterfeited milk were also reported by newspapers [7-8].

To control the quality of milk, the responsible association (Food and Drug Administration) is working very hard by analyzing distributed milk as much as possible. Although low quality milk and counterfeited milk can be detected with the current technologies, only small fraction of milk is sampled and analyzed due to the tremendous amount of milk sold each day. Thus, some counterfeited milk can slip through the analysis to the consumers. This situation is more common in the rural area which sampling and analysis have many limitations. The counterfeiting is much more

dangerous than other problems of the school milk project such as corruption since it directly affects the health of the population. The best example is the melamine incident in 2008 [9]. To solve this problem, both law enforcement system and analysis methods have to be developed. With faster and cheaper analysis methods, more samples can be analyzed and higher safety can be provided to the consumers.

1.2 MILK PROTEIN DETERMINATION

Although there are many methods to detect counterfeiting in milk such as melamine detection [10-15], the absence of any single counterfeiting agent does not guarantee the quality of milk as the milk sample might just be counterfeited by simple water addition. The better solution is the measurement of protein content which is an important nutrient in milk. Any counterfeiting agent added into milk to increase the volume would reduce protein concentration. If the protein concentration is less than the standard, the analyzed milk is certainly low quality milk.

Protein determination is one of the thoroughly studied topics. There are many reliable assays which have been continuously developed for more than ten years [16]. The most notable assay is Kjeldahl method [17], which is accepted by food analysis laboratories as the standard assay for protein determination in milk and other food products (ISO 8968-1, AOAC 991.20). The assay relies on nitrogen in the protein structure. By digestion and distillation, nitrogen can be extracted from sample as ammonia which can be titrated to determine amount of total nitrogen. The protein concentration is then calculated by multiplying the amount of nitrogen with known conversion factor. The Kjeldahl assay has very high accuracy and does not need calibration. However, the assay requires excessive work and long digestion time (at least 20 minutes for milk, AOAC 991.20). The assay is also interfered by non-protein nitrogen-rich substances such as melamine [14-15], which is the cause of melamine incident. It should be noted that other methods that rely on total nitrogen such as combustion method are also affected by melamine.

Spectroscopic assays are good alternative methods for determination of protein concentration in milk. They provide fast and versatile analyses which usually require less time and cost than Kjeldahl assay. Although FT-IR spectroscopy can be used to

quantitatively determine protein concentration as peptide bond expresses amide II band at 1550 cm^{-1} [16], most assays are based on UV-visible spectroscopy. In ultraviolet range, UV-205 and UV-280 methods could be performed as peptide bond gives absorption at 205 nm while aromatic amino acids and cystine disulfide bond give absorption at 280 nm [18-19]. Other methods produce absorption in visible region so they are called colorimetric assays. Biuret test is a well-know assay which produces purple color by copper-proteins complexes. Lowry assay and BCA assay are very similar. While Lowry assay uses the Folin-Ciocalteau reagent to react with Cu^{+} ion, which reduced from Cu^{2+} to form blue color [20], BCA assay uses bicinchoninic acid to form a purple complex with Cu^{+} ion. Ninhydrin assay produces purple color with low protein-to-protein variation, but the assay requires tedious protein digestion. Bradford assay relies on deprotonation of Coomassie Brilliant Blue G-250 via protein binding which yields blue colored products. [18,21] These assays are very interesting since they exhibit color visible to human eye. The visible result raises possibility of naked eye sensing, which is the ultimate goal of easy protein determination. However, these methods still need a spectrometer to be quantitative.

1.3 GOLD NANOPARTICLES AS COLORIMETRIC SENSOR

Gold nanoparticles (AuNPs) are a novel material which has gained much interest in past several years. Due to the chemical stability, high surface area, and distinctive electrical properties, AuNPs have potential in many applications such as SERS substrate [22], conductive ink [23], catalyst [24], cancer therapy [25], etc. The optical property of AuNPs is very remarkable. Small (< 20 nm) AuNPs have red color in their dispersed form but become blue when the particles are aggregated [26]. This proficiency makes AuNPs a very versatile optical sensor. By controlling aggregation/disaggregation of the particles in the presence of target analyte, AuNPs can be applied as naked-eye sensors for specific polynucleotides, specific metal ions, melamine, and other biomolecules [10,15,27-34]. Various strategies such as direct aggregation induced by analyte, functionalization of AuNPs surface to bind with target molecule, or applying competitive binding between analyte and aggregation-inducing agent may be used for sensing [35]. However, the main principle is to create

the difference in the degree of aggregation between when analyte is present and absent. With the AuNPs as sensor, even without spectrometer, quantitative analysis can be performed by comparison of the appeared color and color stripe. Since these assays are inexpensive, do not require complex instrument, and require little analysis time, they are very suitable to be developed into test kit [36].

With many advantages of AuNP-based naked-eye sensing assays, if milk protein determination can be performed in the same way, quality control of milk would be much easier. Much more samples could be tested and the analysis can be done by the consumers themselves. Students in school milk project and individual consumers will be protected from counterfeited and low quality milk.

1.4 THE OBJECTIVE

The objective of this research is to develop a new analysis method of milk protein content using gold nanoparticles. The method has to be simple, rapid, and produces distinctive colors to naked eye.

1.5 SCOPES OF THIS RESEACH

1. Synthesize gold nanoparticles with high concentration and high stability to be used in protein determination assay
2. Find optimum condition (concentration of hydrochloric acid, concentration of gold nanoparticles, and incubation time) for the protein determination assay
3. Investigate the effect of protein concentration, mechanism, and kinetic of the assay

CHAPTER II

THEORETICAL BACKGROUND

2.1 STABILITY OF COLLOIDAL SYSTEMS

In the colorimetric sensing applications, AuNPs are used in colloidal form, mostly in water media. Since the analyses mainly rely on the aggregation of gold nanoparticles, manipulation of particles aggregation is the key of the analysis methods. The aggregation behavior of AuNPs can be explained by theories of colloidal stability.

Solid-in-liquid colloidal systems like AuNPs dispersed in water are called sol, and sometimes suspension. Destabilization of such system has many stages and a lot of technical terms should be explained. Figure 2.1 shows schematic idea of these terms. When particles loss their stability and form loose network with each others, this process is called *flocculation*. If the particles irreversibly tightly packed, the process is *coagulation*. These two processes are two kinds of *aggregation*. However, these three words are often used interchangeably by some authors, so the meaning in some contexts might not strict to the definition [37]. The further step, *coalescence* occurs when the particles fused into bigger particle after coagulation. *Sedimentation* is the separation of particle from the system which normally follows aggregation (but maybe without coalescence) [38].

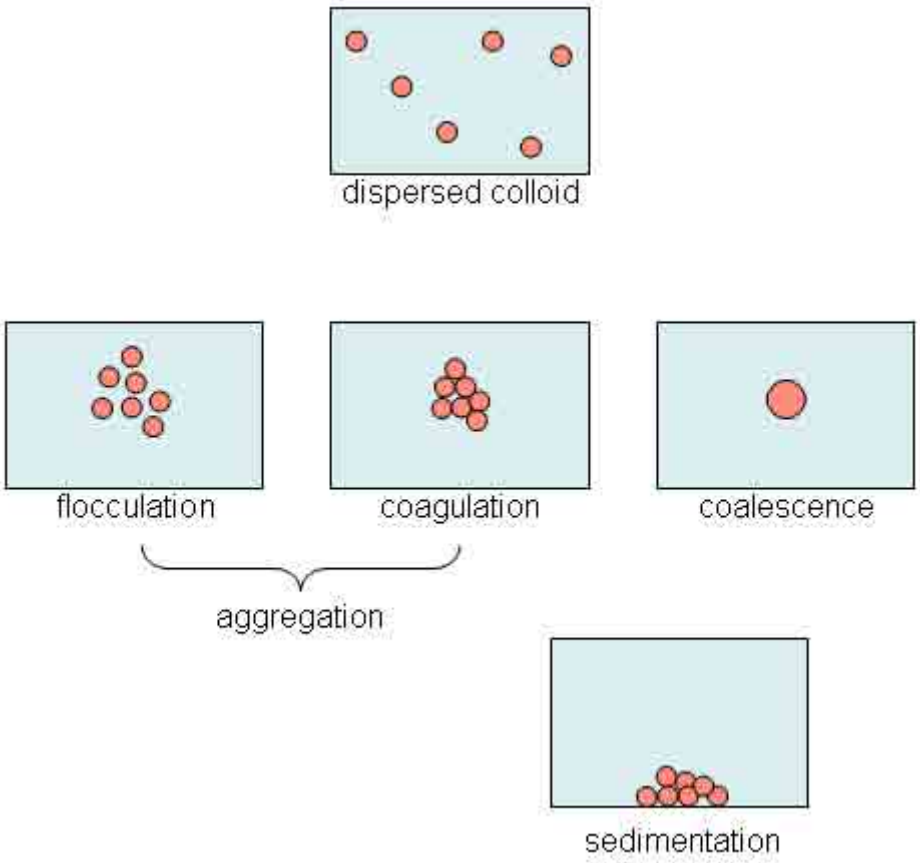

Figure 2.1 Illustration of the destabilization stages for solid-in-liquid colloidal system

A framework of colloid stability can be provided by DLVO theory [39]. In the theory, there are two main forces involved, van der Waals attraction and electrostatic repulsion. The easiest representation of these counteracting forces is to mention them in the term of interaction energy.

$$E_T = E_A + E_R$$

Where E_T is total interaction energy, E_A refers to van der Waals attraction energy, and E_R denotes electrostatic repulsion potential energy. If total energy yields negative value, the particles tend to aggregate.

Since colloid is insoluble by definition, van der Waals attraction between two particles is thermodynamically preferred. The energy of van der Waals interaction in

colloidal system is negative and thus attractive. For two spherical particles, Van der Waals attraction energy is represented by following equation [40-41]:

$$E_A = -\frac{AR}{12D}$$

Where A is Hamaker constant, which equals 3.0×10^{-9} J for gold nanoparticles in water [40]. R denotes radius of the particles while D is the separation distance.

The electrostatic repulsion is a result of repulsion between electric double layers of the two particles. The energy mainly depends on reduced surface potential γ. For two spheres the equation of repulsion energy is [40-41]:

$$E_R = \frac{32\pi\varepsilon\ k^2T^2}{Z^2e^2} R\gamma^2\ exp(-\frac{D}{\lambda_D})$$

Where ε is permittivity of medium, k is Boltzmann constant, T is absolute temperature, Z is charge number of solvated ion, e is electron charge, and λ_D is Debey length.

Surface potential is influenced by ionic strength. In a high ionic strength environment, the electrostatic repulsion is greatly reduced and the particles aggregate easily. This is a strategy used in many gold nanoparticle-based colorimetric assays. By introducing high ionic strength solution to the system, AuNPs aggregate.

In addition to DLVO theory, there is another important factor, the steric repulsion. The repulsion takes place when moderate-to-large molecules are adsorbed on the surface of the particles. Steric interaction energy between two spherical particles with adsorbed layers of thickness L is given by [42]:

$$E_S = \frac{4\pi\ kT\Gamma^2}{3V_m\rho^2}\left(\frac{1}{2}-\chi\right)L\left(1-\frac{D}{2L}\right)^2\left(\frac{3R}{L}+2+\frac{D}{2L}\right)$$

Where Γ is the concentration of adsorbed layer, V_m denotes molar volume of medium, ρ is absolute density of adsorbate, and χ is interaction factor between adsorbate and medium (Flory solvent interaction parameter). If the medium is a good solvent for the adsorbate then χ is less than 0.5 and steric interaction is repulsive. Total potential energy equation, of course, is modified into:

$$E_T = E_A + E_R + E_S$$

Since both electrostatic repulsion and steric repulsion prevents aggregation of the particles. In modern nanoparticle-related researches, molecules that provide these repulsions are often called stabilizers and the ability to provide repulsion force is called stabilization power.

2.2 COLOR OF AGGREGATED GOLD NANOPARTICLES

Color of gold nanoparticles is a result of interaction between electric field of incident light and electron cloud in metal nanoparticles. The phenomenon is called localized surface plasmon resonance. Figure 2.2 illustrates this interaction, light wave has alternating electric field that can affect electrons in gold nanoparticles. Since gold is a conductive material, electrons can propagate in the particles. With the electric field of incident light, electrons are pulled up and down, which cause the oscillation of electron cloud. If frequency of this oscillation corresponds to the frequency of incident light, interaction occurs and the light is absorbed or scattered [43]. For nanoparticles that are much smaller than wavelength of the incident light, the oscillation mostly creates dipole, thus higher multipole can be neglected [44]. For spherical AuNPs with 5 to 20 nm size, this interaction produces an extinction band in visible wavelength and gives red color. The λ_{max} the in UV-visible spectrum of these AuNPs is at about 520 nm.

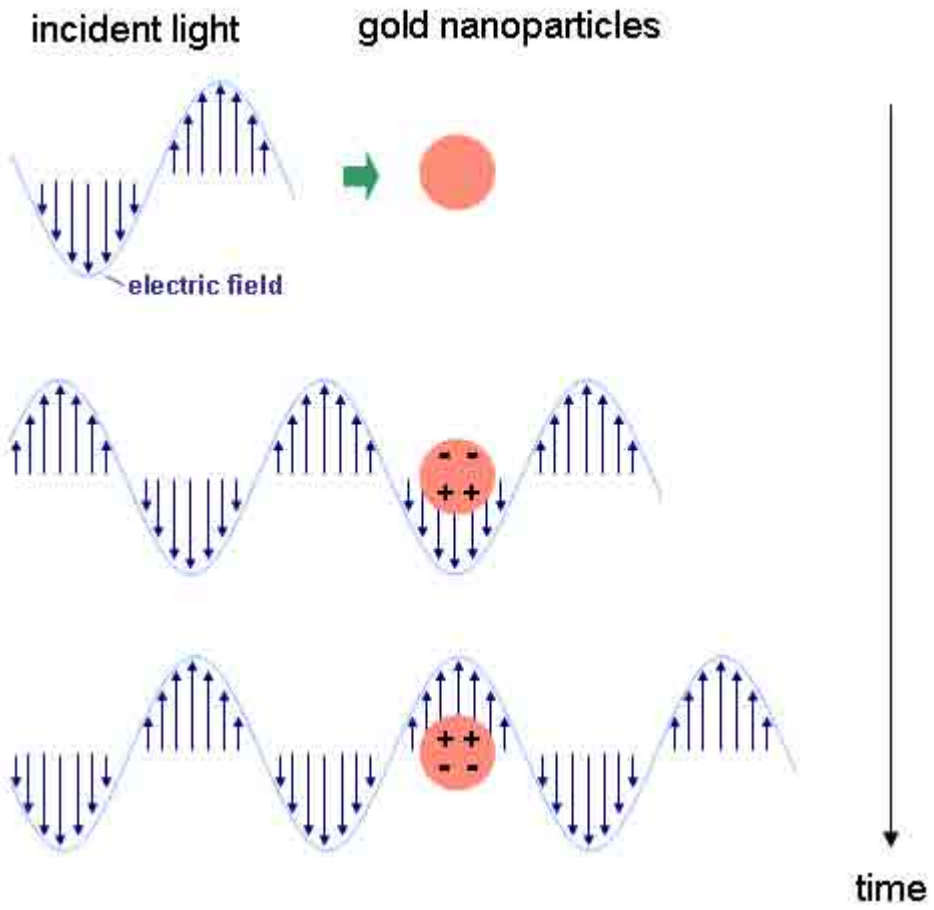

Figure 2.2 Schematic representation of localized surface plasmon resonance in gold nanoparticles

The extinction spectrum of spherical AuNPs can be calculated by Mie solution of Maxwell's equation, which is also known as 'Mie theory' [45]. The parameters for the equation are size of the particles, dielectric constant of the particles, and dielectric constant of the surrounding media. Dielectric constant of gold (and conductive metals) is a complex function of wavelength which can cause difficulty in a manual calculation. However, the calculation can be done quite easily by a computer software. Figure 2.3 shows calculated and real spectrum of 20 nm gold nanoparticles in water. The calculation was done by 'Extinction, Scattering and Absorption efficiencies of multilayer nanoparticles' tool at nanoHUB.com [46] using 1.33 (refractive index of water) as refractive index of surrounding media. The spectrum

calculated by the theory is very accurate, having both λ_{max} and peak shape closely similar to real spectrum.

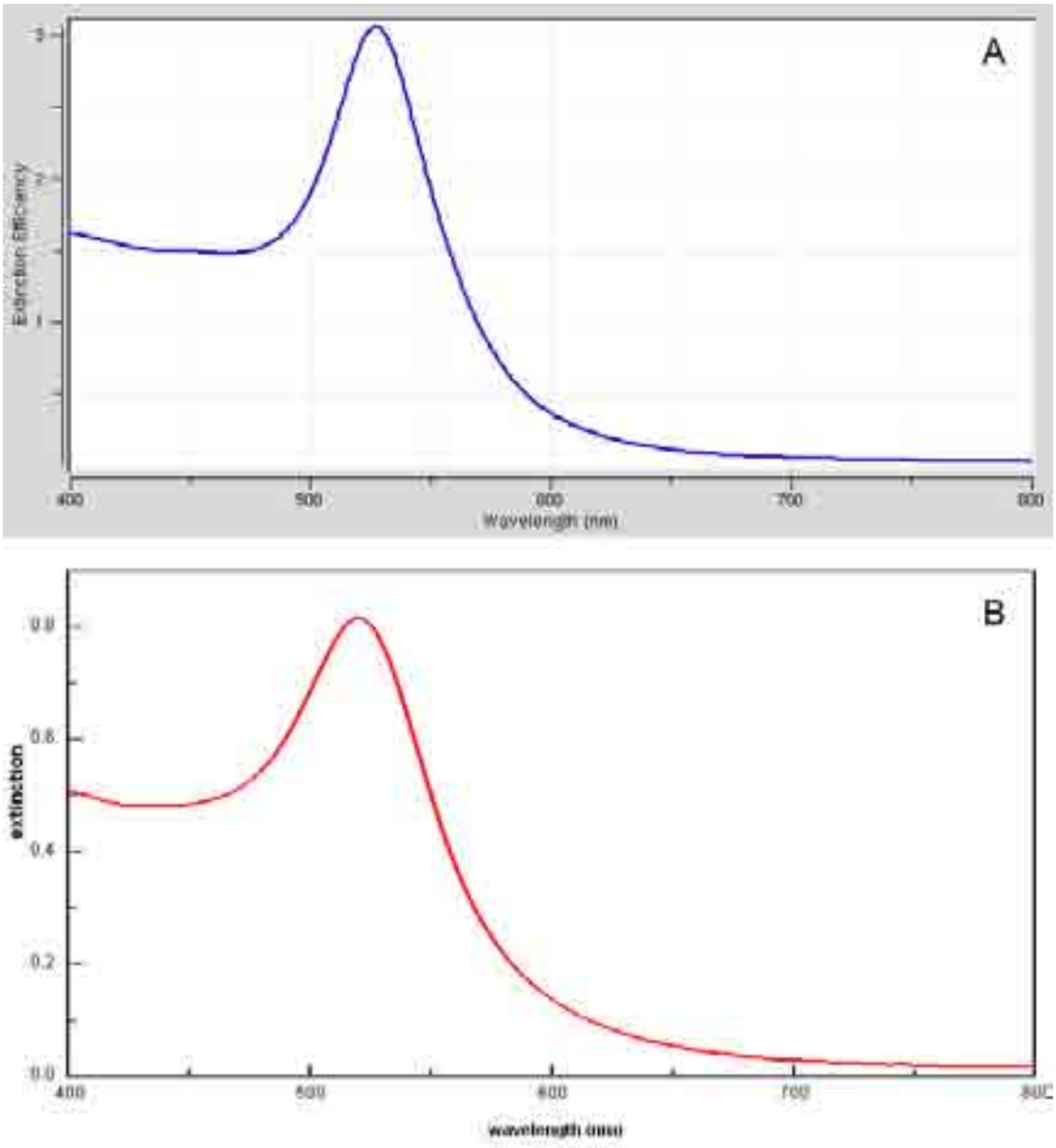

Figure 2.3 (A) Calculated and (B) measured UV-visible spectra of 20 nm gold nanoparticles dispersed in water.

In the aggregated nanoparticles system, localized surface plasmon resonance of nearby particles (distance < 2.5 particle diameter) can interact with each other [47-48]. This interaction, called plasmon coupling, is strongly depended on interparticle

distance [47]. Plasmon coupling between gold nanoparticles has many interesting effects such as electric field enhancement in small area between the particles which can be used in surface enhance raman scattering (SERS) applications [49]. An effect of plasmon coupling, alteration of extinction spectrum, is very important to visual sensing applications. In the effect, new peak emerges at higher wavelength (~ 700 nm) and dominates the spectrum in a fully aggregated system [50]. Figures 2.4 represents the spectra of aggregated AuNPs, compared to dispersed AuNPs. The physical sense of this process can be achieved by plasmon hybridization model [50-51]. In the model, dipole oscillation of two adjacent gold nanoparticles can couple in two modes. For the first mode the dipoles are aligned, resulting in a larger dipole which oscillates at lower frequency so it is responsible for new plasmon resonance peak at longer wavelength. This mode is resembled to bonding orbitals in molecular orbital theory (MO). The second mode of dipole interaction has antialigned dipoles. Since net dipole is zero, this mode has no extinction peak. The latter mode is an analogue of antibonding orbitals in MO. Also, these two modes are orthogonal to each other which is very similar to bonding-antibonding relationship in MO. The simplified diagram of plasmon hybridization is shown in Figure 2.5.

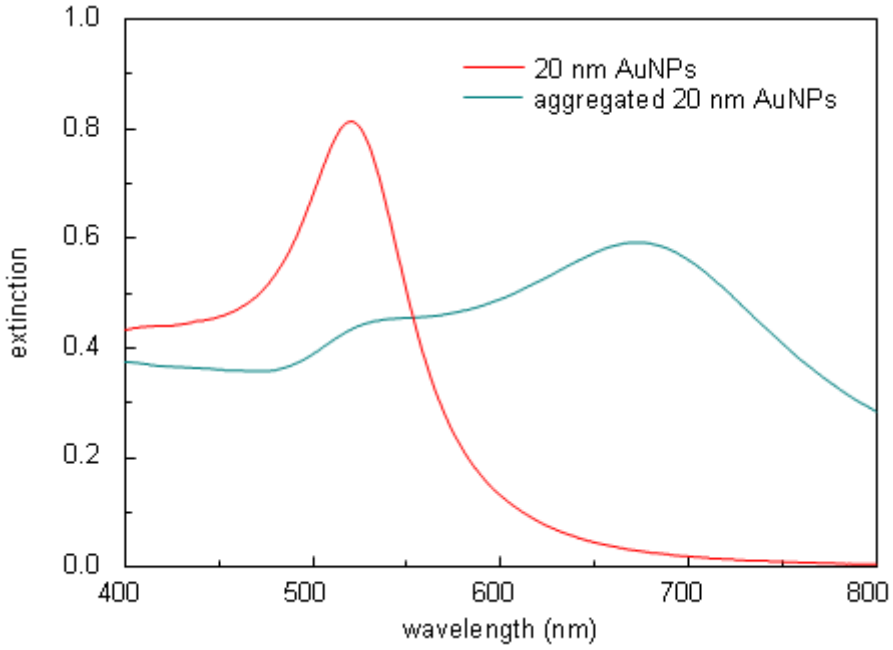

Figure 2.4 UV-visible spectra of dispersed and aggregated gold nanoparticles with the size of 20 nm.

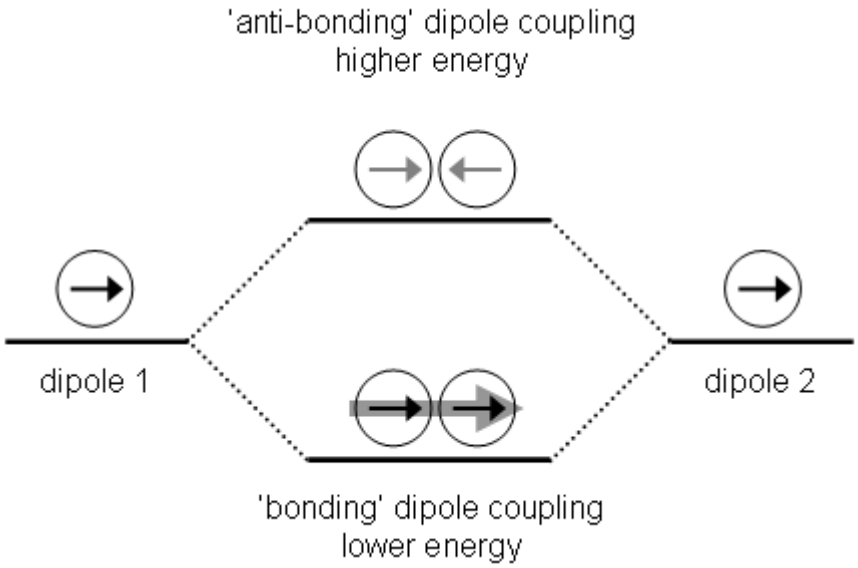

Figure 2.5 Simplified diagram of plasmon hybridization model. The actual diagram has many other modes (such as quadrupole) with higher energy.

Even though spectra of aggregated systems cannot be exactly calculated as in dispersed nanoparticles system, many numerical methods such as finite-difference time-domain (FDTD), discrete dipole approximation (DDA), boundary element method (BEM), etc. can be performed to get a satisfying spectrum [50-52]. Since doubly-aggregated uniform AuNPs system is a special case that was thoroughly studied, data from an empirical method is also available. The λ_{max} of the system can be calculated by this equation [53]:

$$\frac{\Delta\lambda}{\lambda_0} \approx 0.18 \exp\left(\frac{-(D/2R)}{0.23}\right)$$

When $\Delta\lambda$ denotes maxima shift from original spectrum, λ_0 is wavelength at maxima of original peak, D refers to the distance between edges of the particles, and R is diameter of particles.

CHAPTER III

EXPERIMENT

3.1 CHEMICALS AND INSTRUMENTS

Concentrated hydrochloric acid, concentrated nitric acid, sodium hydroxide, sodium borohydride, soluble starch, and bovine serum albumin Fraction V were from Merk. 99.99 % gold pellet was brought from Thailand's Gold Trader Association.

USB4000-UV-Vis from Ocean Optics and UV-Vis-NIR LIGHTSOURCE PH2000 from Mikropack were used to perform UV-Visible spectroscopy. All measurements were done using PMMA cuvette with 0.5 mm path length.

3.2 SYNTHESIS OF STARCH-STABILIZED GOLD NANOPARTICLES

Preparation of 100,000 ppm chloroauric acid ($HAuCl_4$) was done by dissolving 99.99 % gold pellet in aqua regia (3:1 mixture of concentrated HCl and concentrated HNO_3). In detail, 10.00 grams of gold pellet was submerged in 20 mL of DI water and heated to boil. Every five minute, 3 mL of concentrated HCl and 1 mL of concentrated HNO_3 were mixed and then added to the system. The addition of aqua regia was repeated until gold metal was completely dissolved. After that, the solution was being boiled continuously for 3 hours with occasional addition of DI water to prevent the solution from drying. It is important to ensure complete evaporation of HNO_3 and other nitrogen-oxygen compounds since they can disturb the reaction in the following steps. The solution was then adjusted to 100.00 mL.

20 nm starch-stabilized gold nanoparticles were prepared *via* reduction of $HAuCl_4$ by intermediates from alkaline degradation of starch. The method for AuNPs synthesis was developed by Pienpinijtham *et al.* [54]. The procedure in this research was slightly modified from the original. The synthesis was done by boiling 0.5 g of

soluble starch in 50 mL of DI water for 20 minutes. The solution was allowed to cool down to the room temperature and the volume was readjusted to 50.0 mL. The starch solution was reheated to 70°C and 0.250 mL of 0.2 M NaOH was then added to the solution. Meanwhile, 50.0 mL of 2.030×10^{-2} M $HAuCl_4$ with pH adjusted to 6 was mixed with 0.250 mL of 0.2 M NaOH and then heated to 70°C. The two mentioned solutions were mixed together at 15 minutes after the addition of NaOH to starch solution. The suspension initially appeared purplish but gradually became red. The temperature was kept at 70°C for 15 minutes to ensure the completeness of reaction.

Figure 3.1 Apparatus for synthesis of starch-stabilized gold nanoparticles

3.3 PROTEIN CONTENT DETERMINATION ASSAY

The assay of protein determination was performed by simple two-step mixing of the sample, gold nanoparticles, and hydrochloric acid as shown in Figure 3.2. Elaborately, 0.100 mL of diluted milk sample was mixed with 0.100 mL of 1000 ppm AuNPs in 10 mL beaker by vortex mixer. After 3 minutes, 0.800 mL of 2.5 M hydrochloric acid was added and the mixture then underwent vortex mixing for 30 seconds. The UV-visible measurement was done at exactly 3 minutes after the addition of HCl.

Since gold nanoparticles had very high specific absorptivity, the spectrum of the mixture was dominated by AuNPs absorption peak. There was no need of background correction even though milk had some turbidity. Thus, DI water was used as blank in the measurement.

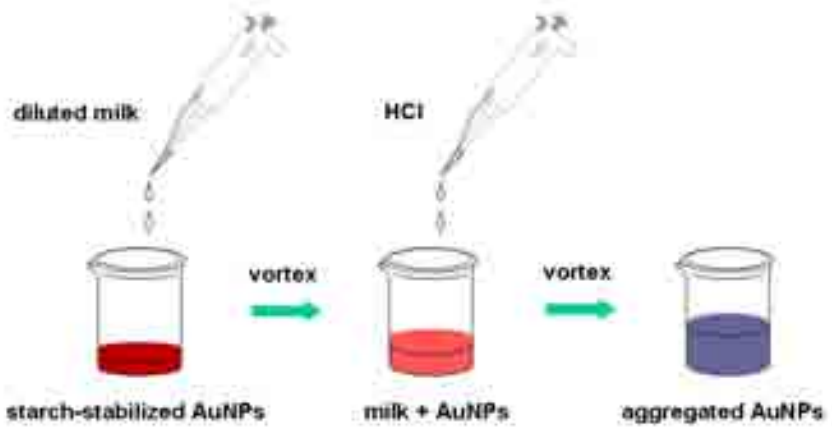

Figure 3.2 Schematic representation of the protein determination assay

To investigate the effect of HCl concentration, 0-3 M HCl were used in the procedure with 400 ppm AuNPs. Using UV-visible spectroscopy, maxima absorption was inspected to find optimal concentration of hydrochloric acid.

Incubation time between milk and AuNPs prior to the addition of HCl was studied by the system with 0.1 % milk, 1000 ppm AuNPs, and 2.5 M HCl. The UV-visible spectra were recorded at 3 minutes after the addition of HCl. The incubation time studied was 0.25, 0.5, 1, 2, 3, 5, 10, and 30 minutes.

Kinetic of the process was also investigated. Using 0.1 % milk, 1000 ppm AuNPs, and 2.5 M HCl hydrochloric acid, the time-dependent spectra were recorded at 1 - 30 minutes after the addition of HCl.

In every study that used milk as sample, Kjeldahl method was used as reference method to determine the exact protein concentration. Every step of sample preparation and measurement was done without extraction of protein or lipid from milk.

3.4 METHOD VALIDATION USING STANDARD PROTEIN

To ensure that it was protein (and not other components in milk) which played role in the inhibition of gold nanoparticles aggregation, bovine serum albumin was used as standard protein to test the system.

In the detail, 0.300 g of BSA was dissolved in 100.00 mL of DI water to make 3.00 mg/mL solution. Then, 0.100 mL of the solution was mixed with 0.100 mL of 1000 ppm AuNPs. After 3 minutes of mixing, 0.800 mL of 2.5 M HCl was then added. UV-visible spectrum measurement was done after another 3 minutes. The solution of $3.00x10^{-1}$, $3.00x10^{-2}$, $3.00x10^{-3}$, and $3.00x10^{-4}$ mg/mL concentration were prepared by successive dilution and then used as samples in the same assay.

3.5 EFFECT OF INTERFERING SUBSTANCES

0.2 M lactose solution, 2 % table sugar solution, 0.02 M melamine solution, and 0.2 M NaCl solution were prepared by dissolving 1.802 g of lactose monohydrate, 1 g of table sugar, 0.063 g of melamine, and 0.292 g of sodium chloride in 25 mL DI water. 2 % starch solution was prepared by boiling 1.00 g of soluble starch in 50 mL DI water for 15 minutes.

The effect of interfering substances on the assay was studied for both with and without the presence of milk protein. 500 μL of each interfering substance was mixed with 100 μL of 1 % milk and 400 μL DI water. The 100 μL of the mixed solution was then used as sample in the 1000 ppm AuNPs assay. For the batches without milk protein, 1 % milk was omitted and 500 μl DI water was added instead of 400 μL. The results were compared with the results of the assay with 1 % milk and 0.1 % milk.

CHAPTER IV

RESULTS AND DISCUSSION

4.1 GOLD NANOPARTICLES SYNTHESIZED *VIA* GREEN SYNTHESIS USING STARCH AS REDUCING AGENT

There are two requirements for gold nanoparticles to be an appropriate colorimetric sensor for this research, red color and high concentration. The former property is needed because only red gold nanoparticles can give distinctive color changing phenomenon, which we will discuss later, while the latter provides high sensitivity and wide range of adjustment to the system. Therefore, we chose green synthesis method of Pienpinijtham et. al. to prepare the gold nanoparticles since the method is capable for both red color and high (up to 1000 ppm) concentration.

Synthesized gold nanoparticles have deep red color and 1000 ppm concentration. The UV-Visible spectrum shows a peak at 519 nm which is the characteristic peak of gold nanoparticles with ~20 nm size.

The completeness of reaction can be examined by the addition of sodium borohydride. The chemical is a strong reducing agent that can reduce any remaining gold ion. Thus, there would be a change in plasmon extinction band if the reaction was not complete. In our system, since borohydride test indicated that no significant change in UV-visible spectrum, the reaction was certainly complete.

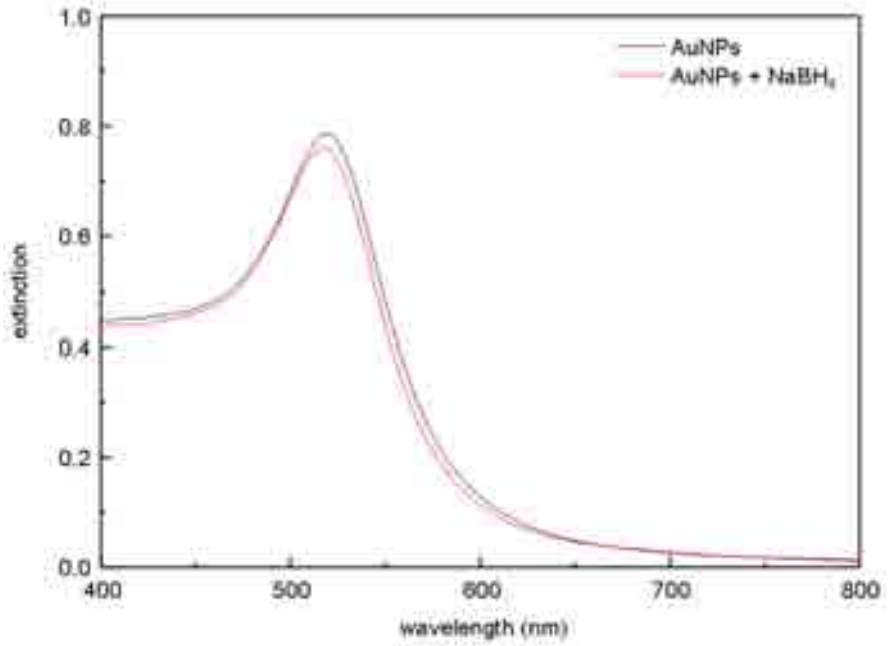

Figure 4.1 Spectra of gold nanoparticles used in this work. The addition of sodium borohydride did not significantly affect the spectrum.

Dynamic light scattering and transmission electron microscopy (TEM) were used to investigate size of the nanoparticles. Average size of gold nanoparticles from these two techniques was 23 nm and 25 nm, respectively.

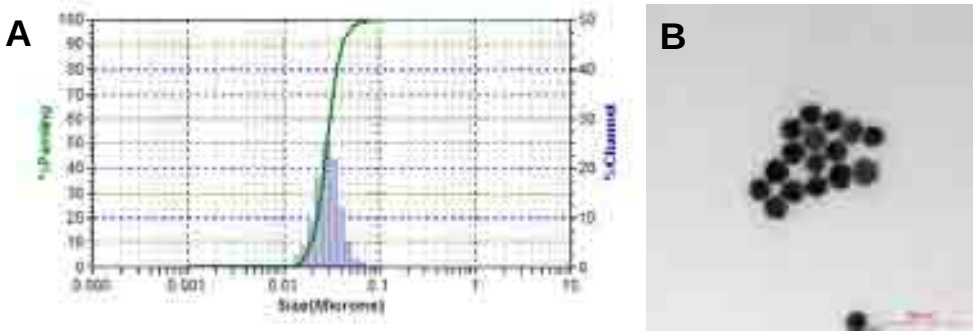

Figure 4.2 The representation of gold nanoparticles size: (A) size distribution graph from dynamic light scattering and (B) TEM image.

To examine stability of the nanoparticles, another batch of AuNPs was kept at room temperature and dark environment. UV-visible spectra were measured at one week and eight months after the synthesis. The spectra show that the suspension did

not undergo major transformation. Naked-eye observation found only little sedimentation of the particles on the bottom of container and no significant color change. It can be concluded that the AuNPs were stable at room temperature.

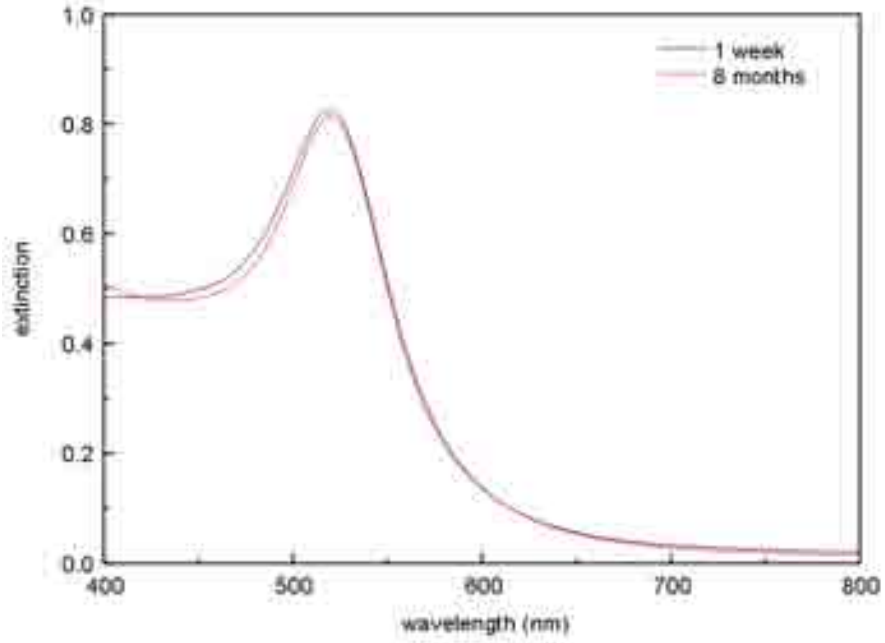

Figure 4.3 UV-visible spectra of AuNPs measured at 1 week and 8 months after the synthesis.

4.2 MILK PROTEIN DETERMINATION ASSAY USING GOLD NANOPARTICLES AS COLORIMETRIC SENSOR

4.2.1 EFFECT OF HYDROCHLORIC ACID CONCENTRATION

In the theory of colloid stability, there are two repulsion forces that separate particles apart, the electrostatic force of electric bilayer and steric repulsion [42]. These forces prevent the particles from aggregation, thus making the colloidal system stable. Since protein acts as a stabilizer which provides steric repulsion, electronic repulsion must be eradicated so the system can be sensitive in probing protein. To accomplish this, enough HCl must be

added to the system. In the experiment, the optimal concentration of HCl was investigated.

The spectra from the assay with 0.2% milk, 400 ppm AuNPs and 0-3 M HCl show that the maxima absorption wavelength sequentially increases from 520 nm to about 590 nm for 0 - 1.5 M HCl concentration. In the 1.5 - 3 M range, the spectra seem very similar despite the increment of HCl concentration. This experiment indicated that the aggregation of gold nanoparticles was complete in the system with 1.5 M or higher concentration of HCl. The colors of solutions also represented the same aspect, with 0 M HCl system appeared red, 0.5 M appeared pink, 1 M appeared purple, and 1.5 - 3 M appeared violet as shown in the inset of Fig 4.4.

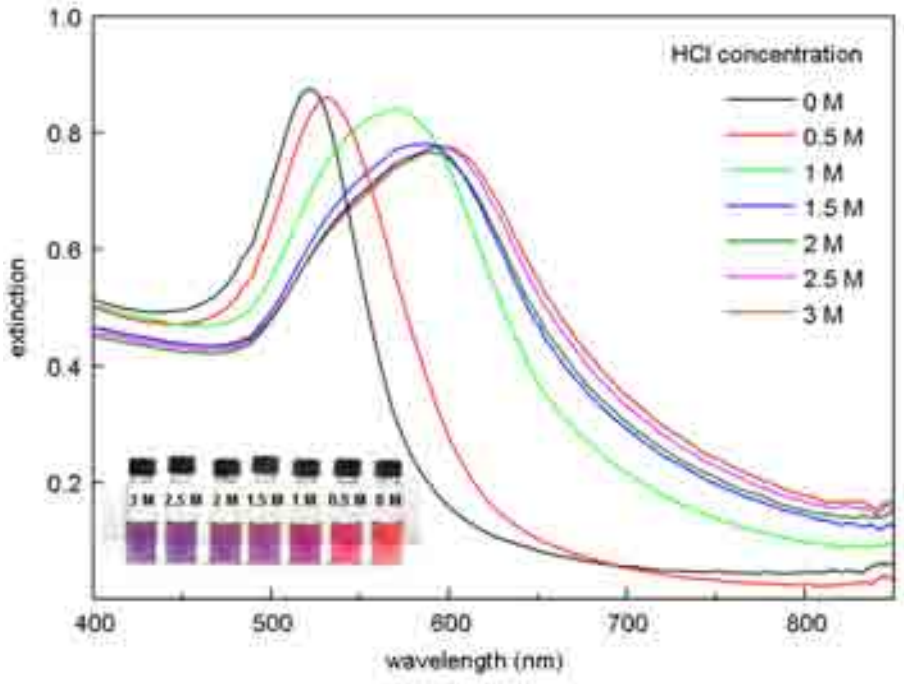

Figure 4.4 UV-visible spectra and images of the system with various HCl concentrations. Both peak shift and color change show optimal trend at 1.5 M.

The same procedure was repeated with 0.10%, 0.20%, and 1.00% milk to determine the effect of HCl for other protein concentrations. As expected,

the results followed similar trend for every milk concentration. The optimal concentration of HCl was around 1.5 M. λ_{max} plot against HCl concentration for each milk concentration is presented in Figure 4.5.

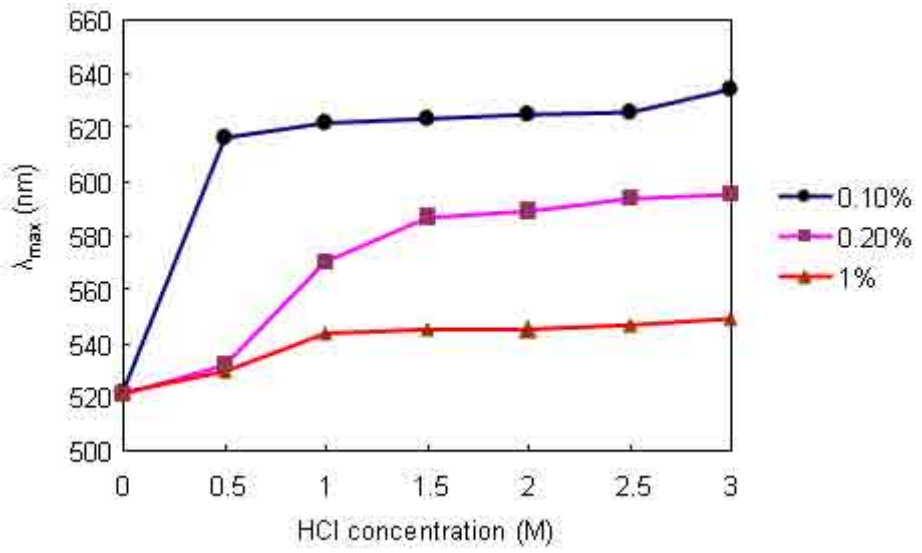

Figure 4.5 λ_{max} of UV-visible spectra from the system with 0.10%, 0.20%, and 1.00% milk and 0 - 3 M HCl concentration

Despite the fact that 1.5 M was the optimal concentration of hydrochloric acid, we chose concentration of 2.5 M for all following experiment to ensure the completeness of interaction.

4.2.2 EFFECT OF INCUBATION TIME BETWEEN MILK AND GOLD NANOPARTICLES

In our system, protein in milk acted as a stabilizer to prevent aggregation of gold nanoparticles. The stabilization by protein came from adsorption of protein on the surface of AuNPs. Since the process of adsorption was not instant, the incubation time between milk and gold nanoparticles before addition of HCl was an important factor. To make the assay reproducible, this duration must be long enough.

The effect of incubation time is presented in Figure 4.6. As the incubation time increases, λ_{max} of the UV-visible spectrum slightly decreases. The low λ_{max} of the batches with longer incubation time indicates that there was less aggregation of AuNPs. This observation can be explained as longer incubation time allowed protein to stabilize AuNPs better. However, this effect is negligible for incubation time longer than 3 minutes.

Another effect which is more important than λ_{max} itself is its variation. Since this value directly implies reproducibility of the assay. In the Figure 4.6, variation of λ_{max} is rather high when HCl was added less than 1 minute after the mixing of milk and AuNPs. This variation is decrease with more incubation time. This effect can be interpreted as the proteins needed a few minutes before effectively stabilized the AuNPs.

Every result mentioned after this was produced with 3 minutes incubation time between milk and AuNPs.

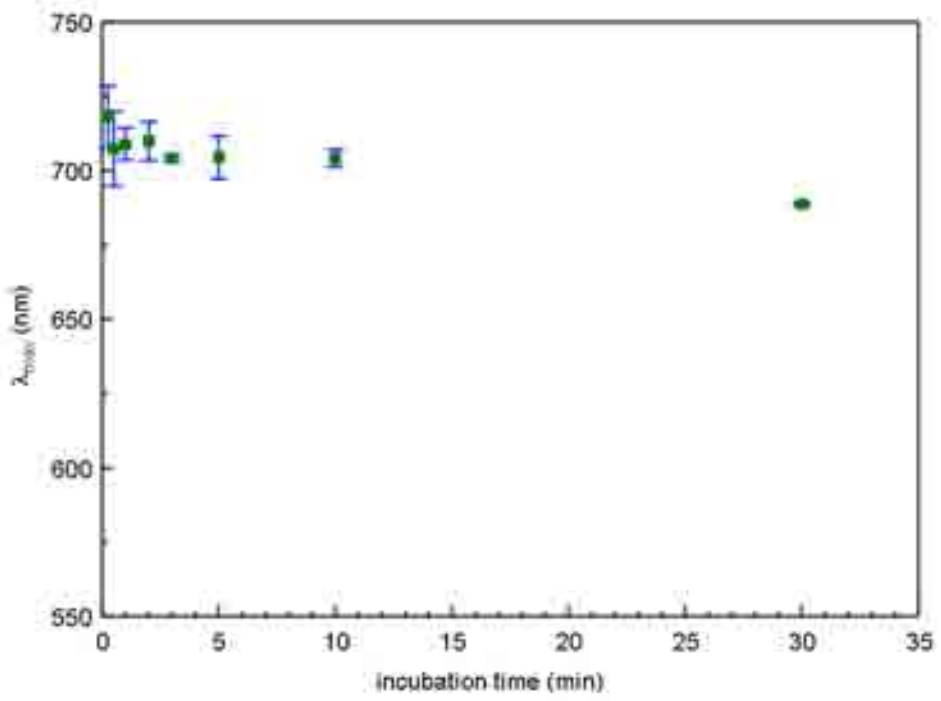

Figure 4.6 λ_{max} of UV-visible spectra from the systems with various AuNPs-milk incubation time

4.2.3 EFFECT OF PROTEIN CONCENTRATION

The effect of protein concentration is the key of this assay since it allows the assay to determine protein content in milk sample. The main principle is that proteins are known to be able to adsorb on gold nanoparticles surface [55], and prevent the aggregation induced by high ionic strength reagent [56-57]. Since the aggregation of AuNPs alters UV-visible spectrum [10,50], the degree of aggregation can be measured by colorimetric measurement. Thus, protein concentration can be evaluated. Figure 4.7 displays schematic representation of the strategy.

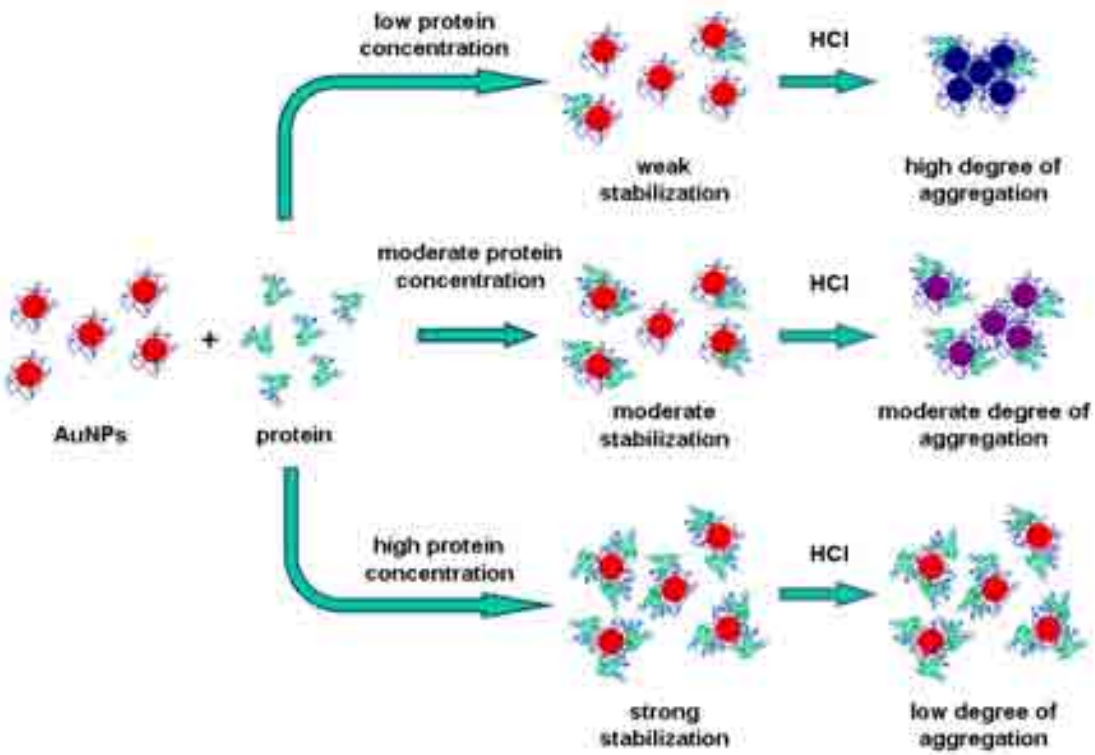

Figure 4.7 Schematic representation of the strategy of the assay. Protein concentration can be determined *via* aggregation degree of gold nanoparticles.

The result is as expected, the assay could distinguish milk with different protein concentration. The spectra and images of each system are shown in Figures 4.8, 4.9, and 4.10.

From the spectra in Figure 4.8, every system shows the same trend, with higher concentrations of milk give lower λ_{max}. Since the λ_{max} shifts by a great degree between each concentration (even more than 100 nm in some range), the system can be easily used to estimate protein concentration in milk. The colors of the mixtures were very distinguishable so naked-eye sensing was also possible. For the 1000 ppm AuNPs systems, results from milk with 10, 100, 1000, 10000, 100000 dilution factor and blank (2.93, 2.93×10^{-1}, 2.93×10^{-2}, 2.93×10^{-3}, 2.93×10^{-4}, 0 mg/mL protein equivalents) have λ_{max} at 535, 553, 708, 809, 833, and 843 nm respectively. Colors of the mixtures were red, violet, and blue for 1:10 to 1:1000 diluted milk and grayish blue for the rest as represented in Figure 4.9.

It was the interparticle plasmon coupling which responsible for color change of the particles. AuNPs with 20 nm size would normally have plasmon extinction peak at 520 nm and appear red. However, when the particles aggregate, a new extinction peak of the interparticle plasmon coupling will appear. This new peak usually appears at 650 nm or higher wavelength. Interparticle plasmon coupling also reduces the intensity of the original peak of gold nanoparticles at 520 nm [48,50,52].

Kim et. al. [26] demonstrated with citrate-capped AuNPs that the interparticle plasmon coupling peak would get redshifted and gain intensity as the degree of aggregation increase. In the system with high degree of aggregation, the extinction peak shift to red-infrared region so the particles appear as blue or grayish color. This was exactly observed in our low protein concentration system, as low stabilization power could prevent aggregation only slightly and the mixture appeared blue to gray.

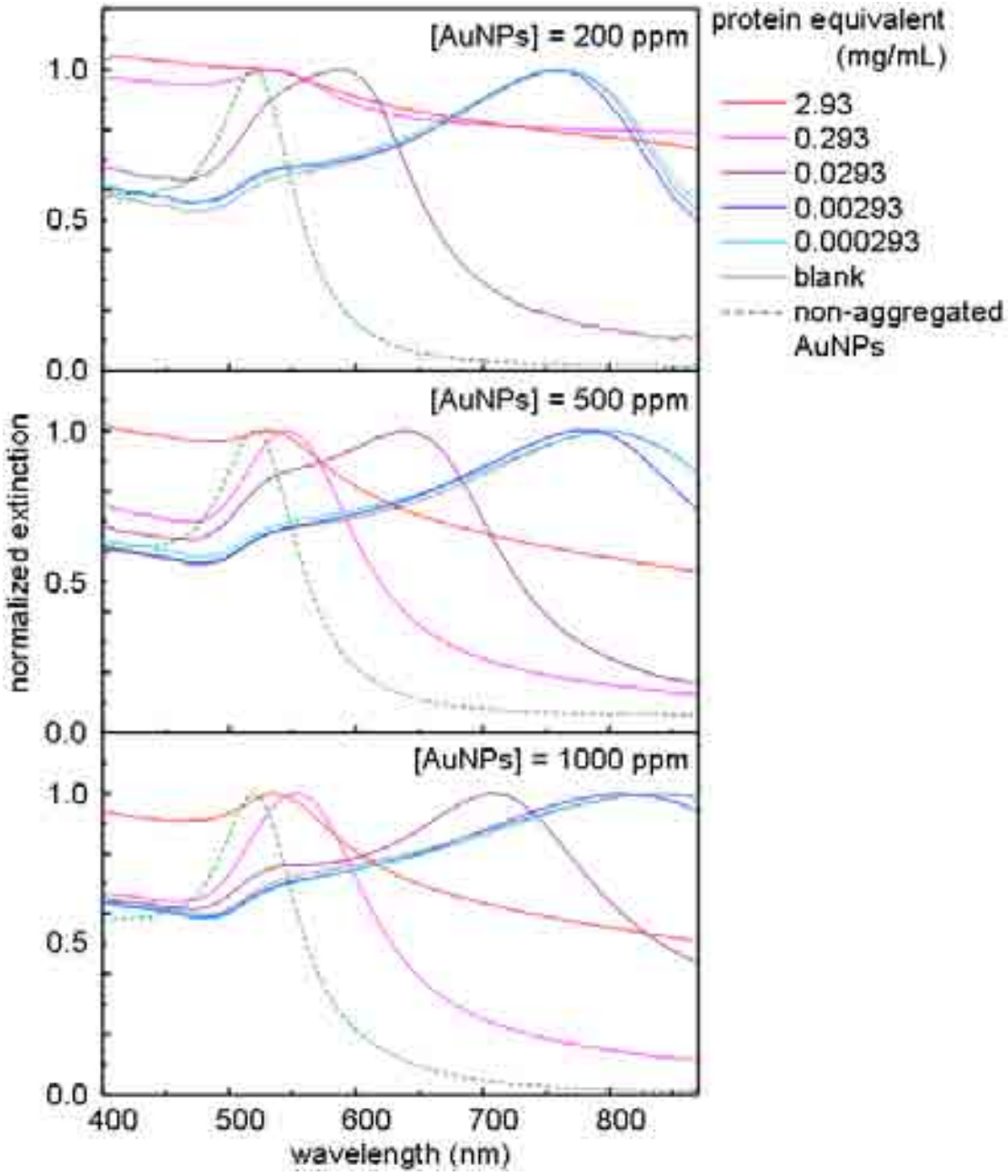

Figure 4.8 UV-visible spectra of 200, 500, and 1000 ppm AuNPs after the addition of HCl in the system with 10 to 100,000 dilution factor of milk (2.93 to 2.93 x 10^{-4} mg/mL protein equivalent)

Figure 4.9 Image of the systems with 1000 ppm AuNPs and milk with (A) 1, (B) 10, (C) 100, (D) 1000, (E) 10000, (F) 100000 dilution factor, and (G) without milk

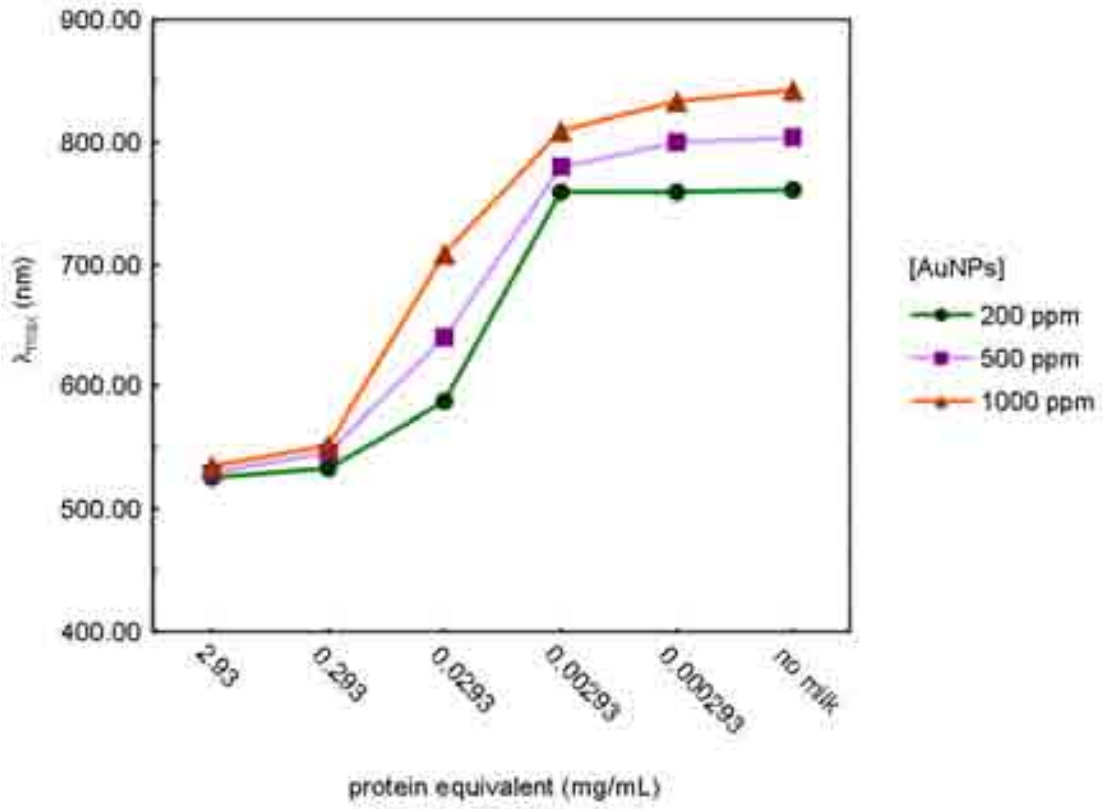

Figure 4.10 λ_{max} from UV-visible spectra of 200, 500, and 1000 ppm AuNPs after the addition of HCl in the system with 10 to 100000 dilution factor of milk (2.93 to 2.93 x 10^{-4} mg/mL protein equivalent)

Figure 4.10 shows another important aspect. The concentration of AuNPs also affects the λ_{max} of the final mixtures. Generally, the spectra from the system with high AuNPs concentration have higher λ_{max} than the spectra of the system with lower AuNPs concentration. The systems with $2.93x10^{-2}$ mg/mL protein are good examples, with λ_{max} at 587, 639, and 708 nm for 200, 500, and 1000 ppm of AuNPs respectively. However the effect is not identical for every protein concentration. While AuNPs concentration greatly affects the λ_{max} for $2.93x10^{-2}$ mg/mL protein, the λ_{max} for $2.93x10^{-1}$ and $2.93x10^{-3}$ mg/mL systems are far less influenced. This phenomenon made systems with 1000 ppm AuNPs sensitive in $2.93x10^{-1}$ to $2.93x10^{-2}$ mg/mL protein range and 200 ppm AuNPs sensitive in $2.93x10^{-2}$ to $2.93x10^{-3}$ mg/mL protein range (as shown in Figure 4.9). Therefore, this colorimetric assay can provide an adjustable effective range by using various AuNPs concentrations.

To emphasize the sensitivity of 1000 ppm AuNPs for the $2.93x10^{-1}$ to $2.93x10^{-2}$ mg/mL protein range, diluted milk with $2.81x10^{-2}$, $5.62x10^{-2}$, $8.43x10^{-2}$, $1.12x10^{-1}$, $1.41x10^{-1}$, $1.69x10^{-1}$, $1.97x10^{-1}$, $2.25x10^{-1}$, and $2.53x10^{-1}$ mg/mL protein was tested by the assay. Figure 4.11 represents the spectra. It is clearly seen that the peak of plasmon extinction undergo redshift as the protein concentration decreases. Since the shift is very large in this concentration range (from 560 nm of $2.53x10^{-1}$ mg/mL to 682 nm for $2.81x10^{-2}$ mg/mL protein), the change of color was easily recognizable. As the colors shifted from red to blue in just an order of magnitude of dilution, the assay is confirmed to be sensitive for this range. Although the relationship of λ_{max} and protein concentration is not linear, the linearity can be achieved in the plot of extinction ratio at maxima and 520 nm against protein concentration. This linear plot can be used as calibration curve for quantitative determination of protein content.

Since the assay with 200 ppm AuNPs concentration also has it own sensitive range in $2.93x10^{-3}$ to $2.93x10^{-2}$ mg/mL protein concentration, diluted milk with protein concentration of $2.81x10^{-3}$, 5.62×10^{-3}, $8.43x10^{-3}$, $1.12x10^{-2}$, $1.41x10^{-2}$, $1.69x10^{-2}$, $1.97x10^{-2}$, $2.25x10^{-2}$, $2.53x10^{-2}$, and $2.81x10^{-2}$ mg/mL was examined by the assay. The result is similar to the result from 1000 ppm AuNPs but the extinction of the UV-visible spectra is much lower due to low

AuNPs concentration. Although the plot of extinction ratio at maxmia and at 520 nm against the protein concentration is not linear, the difference of appeared colors was visible for naked eye. By sensing the color, semi-quantitative estimation of protein concentration can be performed.

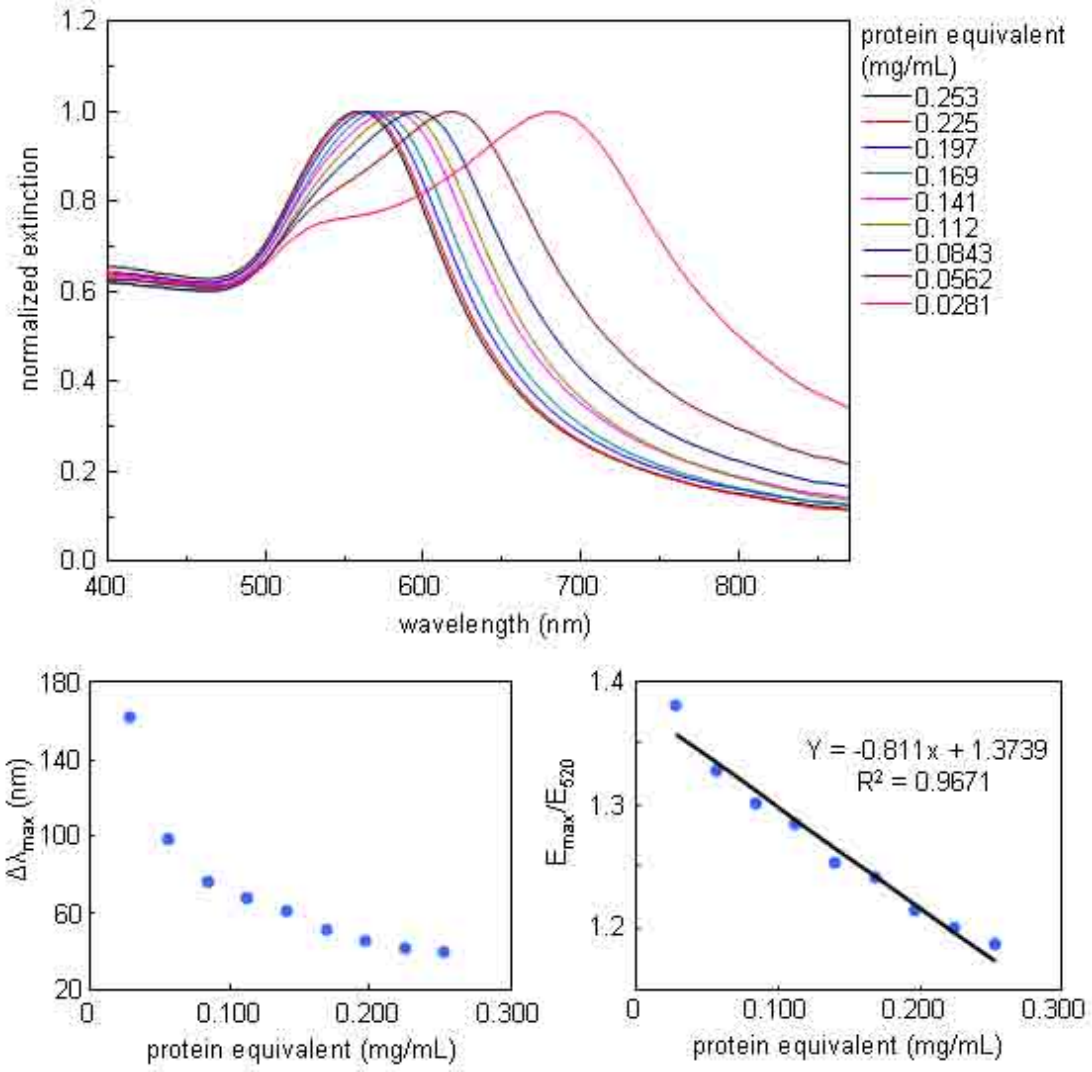

Figure 4.11 UV-visible spectra, $\Delta\lambda_{max}$ against protein concentration plot ($\Delta\lambda_{max}$ is defined as λ_{max} - 520), and extinction ratio between at maxima and 520 nm against protein concentration plot of the results in 2.81×10^{-2} to 2.53×10^{-1} mg/mL protein range.

One interesting point to be mentioned is that there is no need of lipid extraction for this assay. As turbidity of lipid micelle in milk can hinder the

spectrum peak in colorimetric assay, many protein determination methods usually require extraction of the lipid micelle. Some techniques, such as Bradford assay are very sensitive so the absorption peak of the bradford reagent overrides the turbidity [58]. Gold nanoparticles in this assay, with high molar extinction coefficient of 1 x 10^9 M^{-1} cm^{-1}, can give strong absorption peak which undoubtedly rules against extinction from turbidity of lipid micelle. This extinction coefficient is about 1000 times of typical organic dyes. [59]

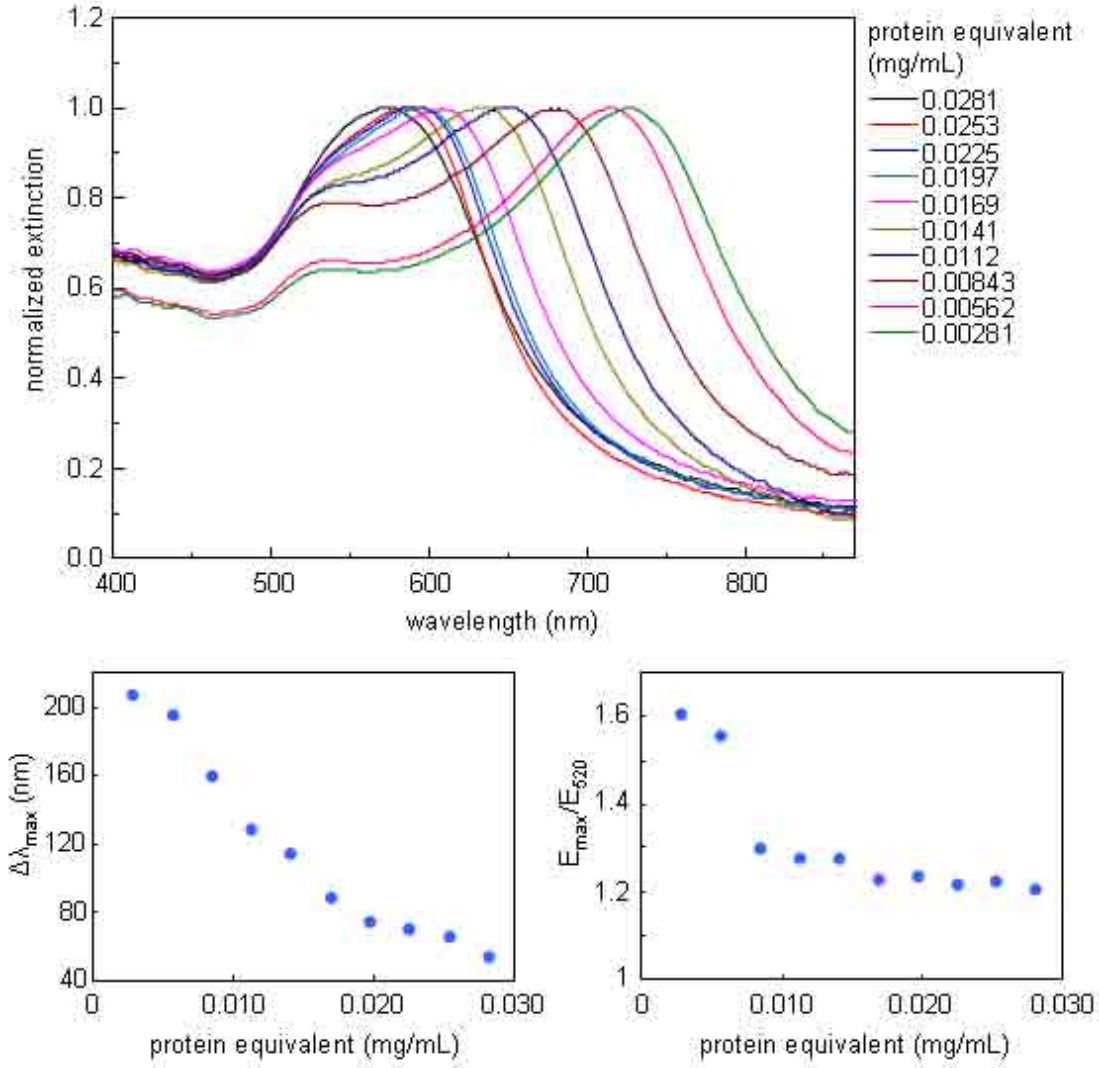

Figure 4.12 UV-visible spectra, $\Delta\lambda_{max}$ against protein concentration plot ($\Delta\lambda_{max}$ is defined as λ_{max} - 520), and extinction ratio between at maxima and 520 nm against protein concentration plot of the results in 2.81x10^{-3} to 2.81x10^{-2} mg/mL protein range.

4.2.4 KINETIC STUDY OF THE ASSAY

Analysis time is an important factor for analysis methods for the mass products since less time required to practice allows more samples to be examined. This factor is even more important for products with short lifespan such as fresh milk. To optimize the measurement time, kinetic study of the system with 1000 ppm and 0.1% milk ($2.93x10^{-2}$ mg/mL protein) was performed. Figure 4.13 suggests that after the fast interaction in the first minute, the aggregation rate became slow as the λ_{max} only increase slightly. The λ_{max} seems to be steady at around the tenth to twentieth minute. Although the tenth minute would be a nice time of measurement, the UV-visible spectra shows that the peak losses its extinction every minute. This extinction loss is a result from particles sedimentation. As some aggregate precipitates to the bottom of the container, the number of particles in the suspension is reduced and the extinction decreases. At the tenth minute, the peak already losses about 20% extinction and it would loss another 20% at twentieth minute. The decrement of extinction is not favorable because it reduces the resolution of the assay. As a consequence, the third minute was chosen as the time of measurement. At the time, the peak has already passed through quick change of the first minute and the intensity was still high.

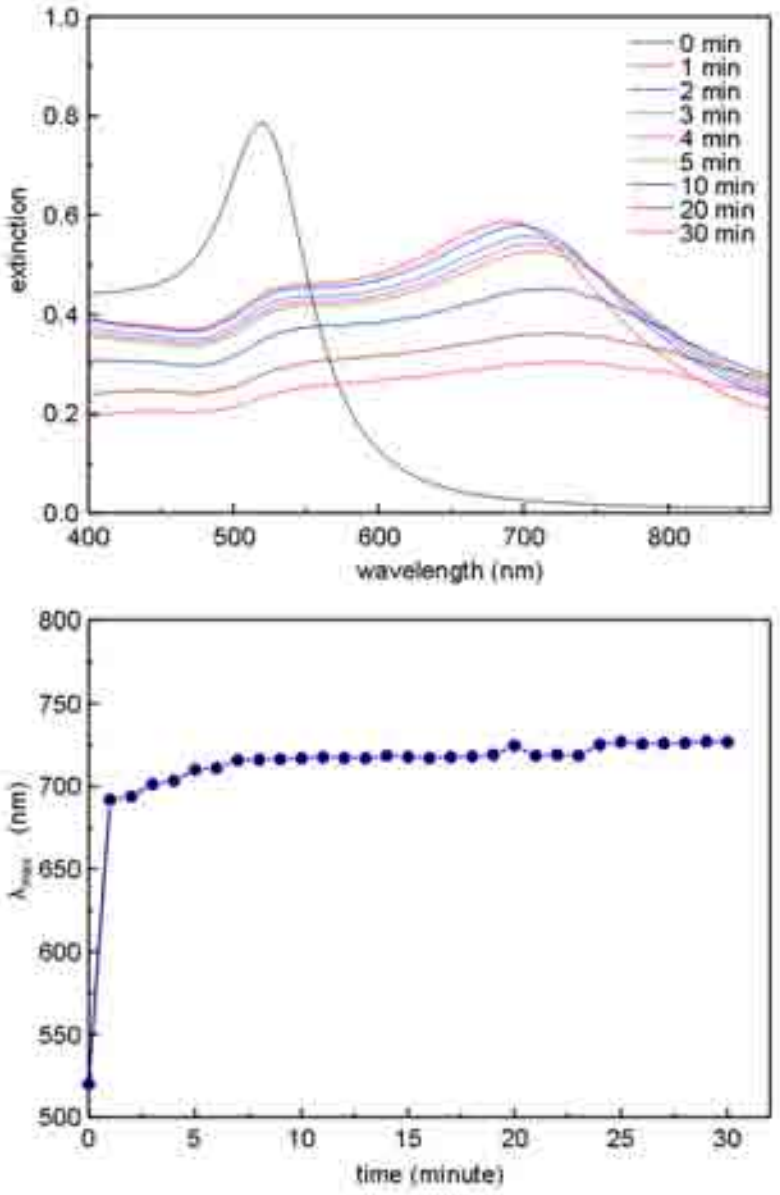

Figure 4.13 UV-visible spectra and λ_{max} vs time plot of the kinetic study using 1000 ppm AuNPs and 0.1% milk system. The time mentioned in the plot is the time after the addition of HCl.

4.3 METHOD VALIDATION USING STANDARD PROTEIN

Since there are many constituents in milk such as protein, lactose, fat globule, and vitamins, it is not conclusive that protein was responsible for the AuNPs stabilization without further validation. The possible way to prove that the stabilization was provided by protein is to extract milk sample so that only milk protein left and perform the assay. However, the process of extraction requires many steps and does not give 100% yield. Thus, another much more comfortable pathway was chosen. The procedure was to use commercially available pure protein in the assay. In this experiment we chose bovine serum albumin (BSA) as a standard protein. Although BSA is not a milk protein, it has similar amino acids component to the beta-lactoglobulin [60] which is the major soluble protein in milk.

The result in Figure 4.14 suggests that BSA could inhibit the aggregation of AuNPs as the higher concentration of BSA could prevent the alteration of extinction peak from original position at 520 nm. The colors of mixtures with high to low BSA concentration also had usual color trend of red, pink, violet, blue, and grayish blue as similar to the test with diluted milk. Both UV-visible spectra and visual observation supports the hypothesis that it was protein which stabilized the AuNPs.

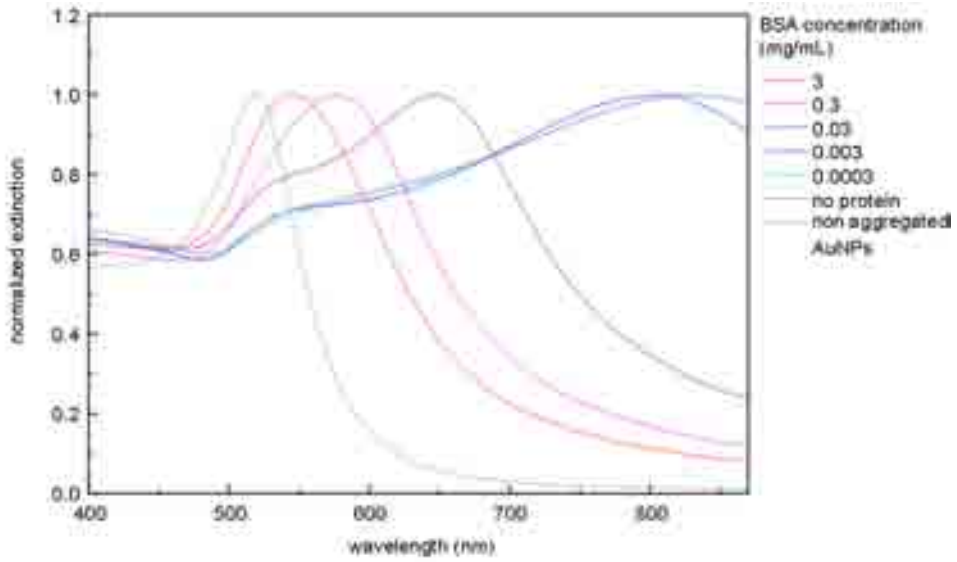

Figure 4.14 UV-visible spectra of the assay with 3.00 to 3.00×10^{-4} mg/mL BSA

4.4 EFFECT OF INTERFERING SUBSTANCES ON THE ASSAY

Because the assay is developed to determine the quality of milk, it would be normal if some of the samples are counterfeited. Hence, the study of counterfeiting tolerance of the assay must be done to assure that the assay will be working under the condition. Therefore, we studied the effect of five interfering substances, namely starch, lactose, table sugar, melamine, and sodium chloride. The reason that we chose these substances is because they are potentially counterfeiting agents. Starch, table sugar, and sodium chloride are inexpensive ingredients in food industry that are available in mass scale. Melamine was counterfeiting agent of infant formula in the famous melamine incident of China. There is lower possibility for lactose to become counterfeiting agents due to the price and availability, but lactose is already in milk so it should be examine whether it interferes the assay or not.

The result was very satisfying, Figure 4.15 indicates that none of the substance mixed into 0.1% milk (2.81×10^{-2} mg/mL protein) could mimic the result from 1% milk (2.81×10^{-1} mg/mL protein). The UV-visible spectroscopy certainly shows extinction peaks at about 700 nm, suggesting that the interfering substances added did not prevent AuNPs from aggregation. This was expected since sucrose in table sugar and lactose are small molecules which can only provide weak stabilization. Starch has higher stabilization power due to the polymeric structure but it lacks sulfur-contained functional group which binds strongly to gold so its stabilization power is much lower than protein. Sodium chloride in its ion form is even smaller than sugar molecule thus provides no stabilization. Melamine is special, in the UV-visible spectrum it is certain that addition of melamine did not prevent aggregation, but even promoted AuNPs to aggregate. The aggregation of AuNPs by melamine was caused by the multiple amino groups on melamine molecule which can bind to multiple gold particles so the particles are pulled together [15,32].

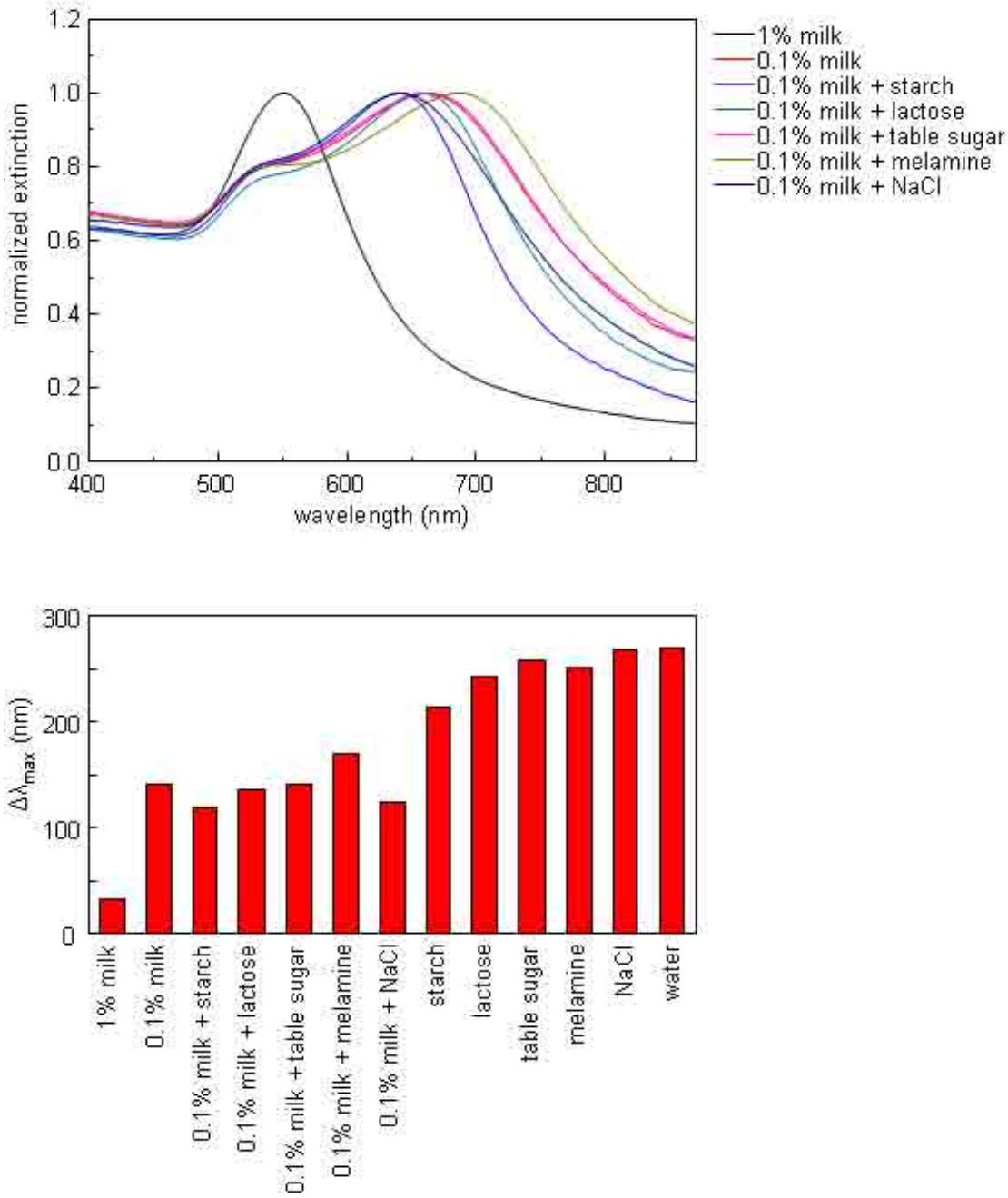

Figure 4.15 UV-visible spectra and $\Delta\lambda_{max}$ plot of the results from the assay with 1% milk, 0.1% milk and each interfering substance. $\Delta\lambda_{max}$ is defined by $\Delta\lambda_{max} = \lambda_{max}$ - 520 nm.

With the $\Delta\lambda_{max}$ plot, ones can easily differentiate between high concentration milk and low concentration milk with counterfeiting substance. The result from 1% milk is the only one that gives less than 50 nm $\Delta\lambda_{max}$ while the others have more than

100 nm. In the batches of counterfeiting agent without milk, $\Delta\lambda_{max}$ are even more than 200 nm because there was only little stabilization. However, the $\Delta\lambda_{max}$ of batch with starch is still less than $\Delta\lambda_{max}$ of the assay with DI water (268 nm) because weak stabilization of the substance can slightly prevent the aggregation.

Visual observation was also capable to made distinction between high concentration milk and low concentration milk with counterfeiting substance. 1% milk produced pink color while 0.1% milk produced blue color whether the counterfeiting agents were added or not.

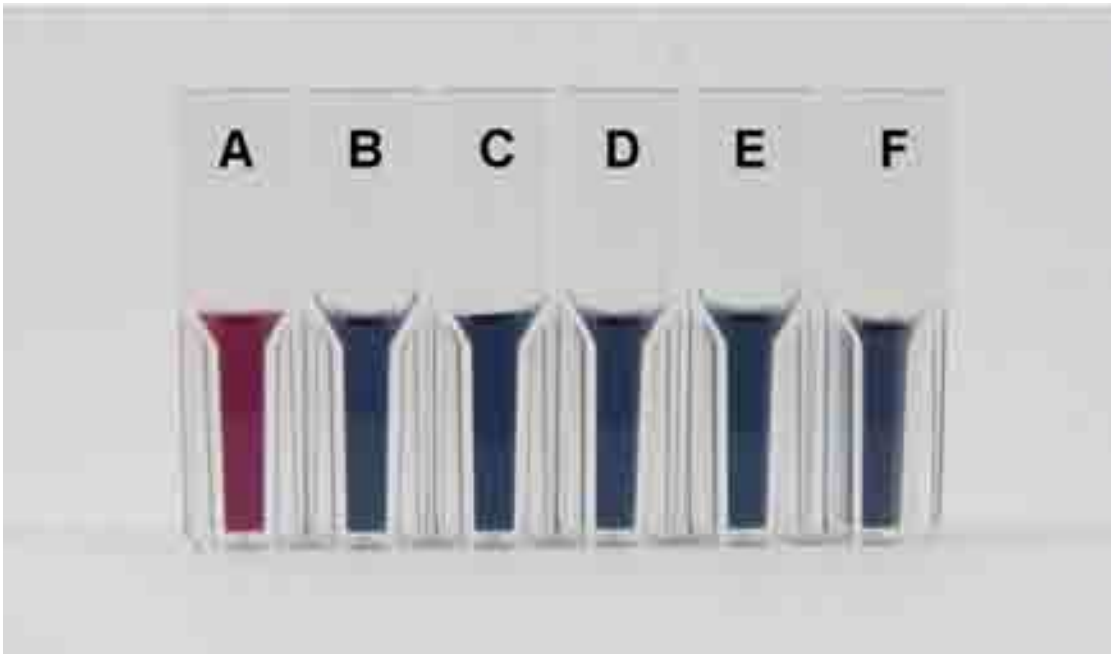

Figure 4.16 Images of the results of the assay with (A) 1% milk, (B) 0.1% milk, (C) 0.1% milk and 1% starch, (D) 0.1% milk and 0.1 M lactose, (E) 0.1% milk and 1% table sugar, and (F) 0.1% milk and 0.01 M melamine

CHAPTER V

CONCLUSIONS

In this research, high concentration starch-stabilized gold nanoparticles were synthesized and used as colorimetric sensor in milk protein determination assay. The particles had ~20 nm size, appeared red, and were stable at room temperature. Synthesized gold nanoparticles were aggregated in contact of hydrochloric acid. However, degree of aggregation could be reduced in the presence of milk protein, depending on protein concentration. Using the phenomenon, assay of milk protein concentration could be formulated. The optimized conditions were found at 2.5 M hydrochloric acid concentration, 3 minutes incubation time, and measurement time at 3 min after addition of hydrochloric acid. The sensitive range of the assay could be adjusted by manipulation of gold nanoparticles concentration, as the assay sensitive in $2.93x10^{-1}$ to $2.93x10^{-2}$ mg/mL protein range for 1000 ppm gold nanoparticles and sensitive in $2.93x10^{-2}$ to $2.93x10^{-3}$ mg/mL protein range for 200 ppm gold nanoparticles. The result could be easily observed by naked-eye sensing as the color appeared red for higher protein concentration and appeared violet-blue for lower protein concentration in the sensitive range. Spectra from UV-visible spectroscopy indicate that the extinction peaks of the batches with high protein concentration are similar to the original gold nanoparticles peak at 520 nm and λ_{max} of the spectra tends to shift to higher wavelength with decreasing protein concentration. For the system with 1000 ppm gold nanoparticles, linear calibration curve (R^2 = 0.9671) can be achieved by plotting extinction ratio between at maxima and at 520 nm against concentration of protein. Five interfering substances (starch, lactose, table sugar, melamine, and sodium chloride) were tested and none of them could alter the result of low concentration protein to appear as high concentration. Thus, the assay can detect milk that was counterfeited by these substances. The assay developed in this research is very easy to practice, can be observed by naked eye, has short analysis time (6

minutes per sample), and does not require extraction process. It is suitable to be developed into a test kit which can be used without the need of expertise.

REFERENCES

[1] เศรษฐกิจการเกษตร, สำนักงาน. สถานการณ์สินค้าเกษตรที่สำคัญและแนวโน้ม ปี 2555. กรุงเทพมหานคร: อักษรสยามการพิมพ์, 2554.

[2] อริยพร โพธิใส. นมโรงเรียนกับการทุจริตในภาครัฐ. วารสารจุลนิติ ฉบับที่ 3 (2552): 127-132.

[3] การเมืองเรื่องนม 'เด็ก'. สยามธุรกิจ (18 กุมภาพันธ์ 2555): 5.

[4] นมปลอมระบาดหนักถึงร้อยละ 70 แนะรัฐเร่งแก้ปัญหานมโรงเรียน. อปท.นิวส์ (7 เมษายน 2553): 18.

[5] ทิพย์วรรณ ปริญญาศิริ, วินัย พุทธกูล, ปาริฉัตร จันทร์ปลั่ง. การสำรวจความพร้อม GMP ของสถานที่ผลิตนมพร้อมดื่มขนาดกลางและเล็ก เพื่อการยกระดับมาตรฐานการผลิตตามเกณฑ์ GMP. วารสารอาหารและยา 2 (พฤษภาคม - สิงหาคม 2546): 48-55.

[6] บุญศรี เลาหภักดี, วรลักษณ์ อนันตกูล, ประภา วุฒิคุณ, วันทนา อ่อนภิรมย์. การศึกษาคุณภาพนมโรงเรียนชนิดพาสเจอร์ไรส์จากแหล่งผลิตจนถึงนักเรียนผู้บริโภคในจังหวัดราชบุรี. วารสารอาหารและยา 1 (มกราคม - เมษายน 2551): 76-84.

[7] เปิดปม 'นมโรงเรียน' ทำไม 'เกษตรกรไทย' ทำอะไรก็จน. พิมพ์ไทย (10 มีนาคม 2552): 7.

[8] เจาะปมนมโรงเรียนคุณภาพต่ำ ใครกัน 'เจริญ' และกลุ่มห้าเสือ ?. ประชาชาติธุรกิจ (2 มีนาคม 2552): 28.

[9] Chan, E.; Griffiths, S.; Chan, C. Public-health risks of melamine in milk products. Lancet 372 (2008): 1444-1445.

[10] Ai, K.; Liu, Y.; Lu, L. Hydrogen-Bonding Recognition-Induced Color Change of Gold Nanoparticles for Visual Detection of Melamine in Raw Milk and Infant Formula. J. Am. Chem. Soc. 131 (2009): 9496-9497.

[11] Tsai, T.; Thiagarajan, S.; Chen, S. Detection of Melamine in Milk Powder and Human Urine. J. Agric. Food Chem. 58 (2010): 4537–4544.

[12] Curcio, M.; Puoci, F.; Cirillo, G.; Iemma, F.; Spizzirri, U.; Picci, N. Selective Determination of Melamine in Aqueous Medium by Molecularly Imprinted Solid Phase Extraction. J. Agric. Food Chem. 58 (2010): 11883–11887.

[13] Desmarchelier, A.; Cuadra, M.; Delatour, T.; Mottier, P. Simultaneous Quantitative Determination of Melamine and Cyanuric Acid in Cow's Milk and Milk-Based Infant Formula by Liquid Chromatography-Electrospray Ionization Tandem Mass Spectrometry. J. Agric. Food Chem. 57 (2009): 7186–7193.

[14] Yin, W.; Liu, J.; Zhang, T.; Li, W.; Liu, W.; Meng, M.; He, F.; Wan, Y.; Feng, C.; Wang, S.; Lu, X.; Xi, R. Preparation of Monoclonal Antibody for Melamine and Development of an Indirect Competitive ELISA for Melamine Detection in Raw Milk, Milk Powder, and Animal Feeds. J. Agric. Food Chem. 58 (2010): 8152–8157.

[15] Chi, H.; Liu, B.; Guan, G.; Zhang, Z.; Han, M. A simple, reliable and sensitive colorimetric visualization of melamine in milk by unmodified gold nanoparticles. Analyst 135 (2010): 1070–1075.

[16] Ribadeau-Dumas, B.; Grappin, R. Milk protein analysis. Lait 69 (1989): 357-416.

[17] Bradstreet, R. Kjeldahl Method for Organic Nitrogen. Anal. Chem. 26 (1954): 185-187.

[18] Ahmed, H. Principles and Reactions of Protein Extraction, Purification, and Characterization. Florida: CRC Press LCC, 2005.

[19] Metsamuuronen, S.; Manttari, M.; Nyström, M. Comparison of analysis methods for protein concentration and its use in UF fractionation of whey. Desalination 283 (2011): 156–164.

[20] Lowry, O.; Rosebrough, N.; Farr, A.; Randall, R. Protein Measurement With The Folin Phenol Reagent. J. Biol. Chem. 193 (1951): 265-275.

[21] Bradford, M. A Rapid and Sensitive Method for the Quantitation of Microgram Quantities of Protein Utilizing the Principle of Protein-Dye Binding. Anal. Biochem. 72 (1976): 248-254.

[22] Dasary, S.; Singh, A.; Senapati, D.; Yu, H.; Ray, P. Gold Nanoparticle Based Label-Free SERS Probe for Ultrasensitive and Selective Detection of Trinitrotoluene. J. Am. Chem. Soc. 131 (2009): 13806–13812.

[23] Maattanen, A.; Ihalainen, P.; Pulkkinen, P.; Wang, S.; Tenhu, H.; Peltonen, J. Inkjet-Printed Gold Electrodes on Paper: Characterization and Functionalization. ACS Appl. Mater. Interfaces 4 (2012): 955−964.

[24] Chen, L.; Hu, J.; Qi, Z.; Fang, Y.; Richards, R. Gold Nanoparticles Intercalated into the Walls of Mesoporous Silica as a Versatile Redox Catalyst. Ind. Eng. Chem. Res. 50 (2011): 13642–13649.

[25] Nam, J.; Won, N.; Jin, H.; Chung, H.; Kim, S. pH-Induced Aggregation of Gold Nanoparticles for Photothermal Cancer Therapy. J. Am. Chem. Soc. 131 (2009) 13639–13645.

[26] Kim, T.; Lee, C.; Joo, S.; Lee, K. Kinetics of gold nanoparticle aggregation: Experiments and modeling. J. Colloid. Interf. Sci. 318 (2008) 238–243.

[27] Beqa, L.; Singh, A.; Khan, S.; Senapati, D.; Arumugam, S.; Ray, P. Gold Nanoparticle-Based Simple Colorimetric and Ultrasensitive Dynamic Light Scattering Assay for the Selective Detection of Pb(II) from Paints, Plastics, and Water Samples. Appl. Mater. Interfaces 3 (2011): 668–673.

[28] Xu, X.; Wang, J.; Jiao, K., Yang, X. Colorimetric detection of mercury ion (Hg^{2+}) based on DNA oligonucleotides and unmodified gold nanoparticles sensing system with a tunable detection range. Biosens. Bioelectron. 24 (2009): 3153–3158.

[29] Dang, Y.; Li, H.; Wang, B.; Li, L.; Wu, Y. Selective Detection of Trace Cr^{3+} in Aqueous Solution by Using 5,5′-Dithiobis (2-Nitrobenzoic acid)-Modified Gold Nanoparticles. ACS Appl. Mater. Interfaces 4 (2012): 1149–1153.

[30] Obare, S.; Hollowell, R.; Murphy, C. Sensing Strategy for Lithium Ion Based on Gold Nanoparticles. Langmuir 18 (2002): 10407-10410.

[31] Qi, Y.; Li, L.; Li, B. Label-free detection of specific DNA sequence-telomere using unmodified gold nanoparticles as colorimetric probes. Spectrochim. Acta A 74 (2009): 127–131.

[32] Wei, F.; Lam, R.; Cheng, S.; Lu, S.; Ho, D.; Li, N. Rapid detection of melamine in whole milk mediated by unmodified gold nanoparticles. Appl. Phys. Lett. 96 (2010): 133702.

[33] Li, B.; Cheng, D.; Mao, L. Visual detection of melamine in raw milk using gold nanoparticles as colorimetric probe. Food Chem. 122 (2010) 895–900.

[34] Basu, S.; Ghosh, S.; Kundu, S.; Panigrahi, S.; Praharaj, S.; Pande, S.; Jana, S.; Pal, T. Biomolecule induced nanoparticle aggregation: Effect of particle size on interparticle coupling. J. Colloid. Interf. Sci. 313 (2007) 724–734.

[35] Wang, Z.; Ma, L. Gold nanoparticle probes. Coordin. Chem. Rev. 253 (2009): 1607–1618.

[36] Zhou, Q.; Liu, N.; Qie, Z.; Wang, Y.; Ning, B.; Gao, Z. Development of Gold Nanoparticle-Based Rapid Detection Kit for Melamine in Milk Products. J. Agric. Food Chem. 59 (2011) 12006–12011.

[37] Schramm, L. Dictionary of Nanotechnology, Colloid and Interface Science. Weinheim, Germany: Wiley-VCH, 2008.

[38] Dickinson, E.; Vliet, T. Food Colloids, Biopolymers and Materials. Cambridge, UK: RSC, 2003.

[39] Verwey, E.; Overbeek, J. Theory of the Stability of Lyophobic Colloids. Ontario, Canada: General Publishing Company, 1999.

[40] Tsai, D.; Pease III, L.; Zangmeister, R.; Tarlov, M.; Zachariah, R. Aggregation Kinetics of Colloidal Particles Measured by Gas-Phase Differential Mobility Analysis. Langmuir 25 (2009): 140-146.

[41] Bhattacharjee, S.; Elimelech, M.; Borkovecb, M. DLVO Interaction between Colloidal Particles: Beyond Derjaguin's Approximation. Croat. Chem. Acta 71 (1998): 883-903.

[42] Ring, T. Fundamentals of ceramic powder processing and synthesis. California: Academic Press, 1996.

[43] Willets, K.; Duyne, R. Localized Surface Plasmon Resonance Spectroscopy and Sensing. Annu. Rev. Phys. Chem. 58 (2007): 267–297.

[44] Hartland, G. Optical Studies of Dynamics in Noble Metal Nanostructures. Chem. Rev. 111 (2011): 3858–3887.

[45] Horvath, H. Gustav Mie and the Scattering and Absorption of Light by Particles: Historic Developments and Basics. J. Quant. Spectrosc. Ra. 110 (2009): 787–799.

[46] Juluri, B.; Huang, J.; Jensen, L. Extinction, Scattering and Absorption efficiencies of multilayer nanoparticles [Online software]. 2010. Available from: http://nanohub.org/resources/nmie [30 March 2012]

[47] Funston, A.; Novo, C.; Davis, T.; Mulvaney, P. Plasmon Coupling of Gold Nanorods at Short Distances and in Different Geometries. Nano Lett. 9 (2009): 1651-1658.

[48] Su, K.; Wei, Q.; Zhang, X. Interparticle Coupling Effects on Plasmon Resonances of Nanogold Particles. Nano Lett. 3 (2003): 1087-1090.

[49] Felidj, N.; Aubard, J.; Levi, G. Discrete dipole approximation for ultraviolet–visible extinction spectra simulation of silver and gold colloids. J. Chem. Phys. 111 (1999): 1195-1208.

[50] Halas, N.; Lal, S.; Chang, W.; Link, S.; Nordlander, P. Plasmons in Strongly Coupled Metallic Nanostructures. Chem. Rev. 111 (2011): 3913–3961.

[51] Nordlander, P.; Oubre, C. Plasmon Hybridization in Nanoparticle Dimers. Nano Lett. 4 (2004): 899-903.

[52] Ghosh, S.; Pal, T. Interparticle Coupling Effect on the Surface Plasmon Resonance of Gold Nanoparticles: From Theory to Applications. Chem. Rev. 107 (2007): 4797-4862.

[53] Jain, P.; Huang, W.; El-Sayed, M. On the Universal Scaling Behavior of the Distance Decay of Plasmon Coupling in Metal Nanoparticle Pairs: A Plasmon Ruler Equation. Nano Lett. 7 (2007): 2080-2088.

[54] Pienpinijtham, P.; Han, X.; Ekgasit, S.; Ozaki, Y. Highly Sensitive and Selective Determination of Iodide and Thiocyanate Concentrations Using Surface-Enhanced Raman Scattering of Starch-Reduced Gold Nanoparticles. Anal. Chem. 83 (2011): 3655–3662.

[55] Glomm, W.; Halskau, O.; Hanneseth, A.; Volden, S. Adsorption Behavior of Acidic and Basic Proteins onto Citrate-Coated Au Surfaces Correlated to Their Native Fold, Stability, and pI. J. Phys. Chem. B 111 (2007): 14329-14345.

[56] Keating, C.; Kovaleski, K.; Natan, M. Protein:Colloid Conjugates for Surface Enhanced Raman Scattering: Stability and Control of Protein Orientation. J. Phys. Chem. B 102 (1998): 9404-9413.

[57] Tran, N.; Wang, T.; Lin, C.; Tsai, Y.; Lai, C.; Tai, Y.; Yung, B. Direct Synthesis of Rev Peptide-Conjugated Gold Nanoparticles and Their Application in Cancer Therapeutics. Bioconjugate Chem. 22 (2011): 1394–1401.

[58] Kamizakea, N.; Goncalvesa, M.; Zaia, C.; Zaia, D. Determination of total proteins in cow milk powder samples: a comparative study between the Kjeldahl method and spectrophotometric methods. J. Food Comp. Anal. 16 (2003) 507–516.

[59] Link, S.; Wang, Z.; El-Sayed, M. Alloy Formation of Gold-Silver Nanoparticles and the Dependence of the Plasmon Absorption on Their Composition. J. Phys. Chem. B 103 (1999): 3529-3533.

[60] Brand, E. Amino Acid Composition of Simple Proteins. Ann. Ny. Acad. Sci. 47 (1946): 187-228.

CURRICULUM VITAE

NAME: Mr. Sanpon Vantasin

DATE OF BIRTH: June 17, 1988 **BIRTH PLACE:** Bangkok, Thailand

ADDRESS: 35/28, Pradijmanutam road, Nuanjan, Buengkum, Bangkok, Thailand 10230
e-mail address: kikujimoji@gmail.com

EDUCATION:

2009	Bachelor of Science (First Class Honors) in Chemistry Chulalongkorn University, Thailand
2011	Master of Science in Chemistry Chulalongkorn University, Thailand

AWARD:

2010	First runner-up in Sci & Tech Innovation and Sustainability Awards (STISA) 2010